HHS Public Access

Author manuscript

Cell Host Microbe. Author manuscript; available in PMC 2020 April 10.

Published in final edited form as:

Cell Host Microbe. 2019 April 10; 25(4): 537–552.e8. doi:10.1016/j.chom.2019.02.003.

Drosophila Histone Demethylase KDM5 regulates social behavior through immune control and gut microbiota maintanence

Kun Chen[#,1,2,3,4], **Xiaoting Luan**[#,1], **Qisha Liu**[#,1,2], **Jianwei Wang**[#,1,2], **Xinxia Chang**[#,1,2], **Antoine M. Snijders**[#,5], **Jian-Hua Mao**[5], **Julie Secombe**[6], **Zhou Dan**[1], **Jian-Huan Chen**[7], **Zibin Wang**[8], **Xiao Dong**[6], **Chen Qiu**[1], **Xiaoai Chang**[3], **Dong Zhang**[1], **Susan E. Celniker**[5], **Xingyin Liu**[*,#,1,2,3,4,9]

[1]Department of Pathogen Biology-Microbiology Division, State Key Laboratory of Reproductive Medicine and Autism research center, Nanjing Medical University, Nanjing 211166, China.

[2]Key Laboratory of Pathogen of Jiangsu Province, Center of global health, Nanjing Medical University, Nanjing 211166, China.

[3]Key Laboratory of Human Functional Genomics of Jiangsu Province, Nanjing Medical University, Nanjing 211166, China.

[4]Key Laboratory of Holistic Integrative Enterology, The Second Affiliated Hospital of Nanjing Medical University, Nanjing 210011, China.

[5]Biological Systems and Engineering Division, Lawrence Berkeley National Laboratory, CA 94720 USA.

[6]Departments of Genetics and Neuroscience, Albert Einstein College of Medicine, Bronx, New York, NY10461, USA.,

[7]Genomic and Precision Medicine Laboratory, Department of Public Health, Wuxi School of Medicine, Jiangnan University, Wuxi 214122, China.

[8]Center for Analysis and Testing, Nanjing Medical University, Nanjing 211166, China.

[9]Lead contact

SUMMARY

[*]Correspondence: xingyinliu@njmu.edu.cn.

AUTHOR CONTRIBUTIONS

X.L conceived project and designed the study; K.C, T.L, X.L, Q.L, W.J, X.C, Z.D, C.Q, Z.W, X.C, J.H.M, J.S and Z.D did experiments; J.C, S.E.C and X.D performed RNA-seq analysis. All authors performed data analyses and interpretations; X.L organized experimentation and wrote a first draft of the manuscript. K.C, A.M.S, X.L and S.E.C generated Figures. X.L, A.M.S, J.H.M, S.E.C and J.S finalized the manuscript.

[#]These authors contributed equally to this work

DECLARATION OF INTERESTS

Authors declare no competing interests.

Loss of function mutations in the histone demethylase KDM5A, KDM5B or KDM5C are found in intellectual disability (ID) and autism spectrum disorders (ASD) patients. Here, we use the model organism *Drosophila melanogaster* to delineate how KDM5 contributes to ID and ASD. We show that reducing of KDM5 causes intestinal barrier dysfunction and changes in social behavior that correlates with compositional changes in the gut microbiota. Therapeutic alteration of the dysbiotic microbiota through antibiotic administration or feeding with a probiotic *Lactobacillus* plantarum L168 partially rescues the behavioral, lifespan and cellular phenotypes observed in *kdm5*-deficient flies. Mechanistically, KDM5 was found to transcriptionally regulate component genes of the Immune Deficiency (IMD) signaling pathway and subsequent maintenance of host-commensal bacteria homeostasis in a demethylase-dependent manner. Together, our study genetically dissects contributing factors of the gut-brain axis influences on animal behavior and suggests modifying the gut microbiome may provide therapeutic benefits for ID and ASD patients.

Abstract

Mutations in members of the *KDM5* gene family are found in intellectual disability and autism spectrum disorder patients. Chen et al. discovered that KDM5-microbiota interactions contribute to animal social behavior. *Drosophila* deficient in *kdm5* display gut dysbiosis, abnormal social behavior, and aberrant immune activation, which *Lactobacillus plantarum* L168 administration can improve.

Graphical Abstract

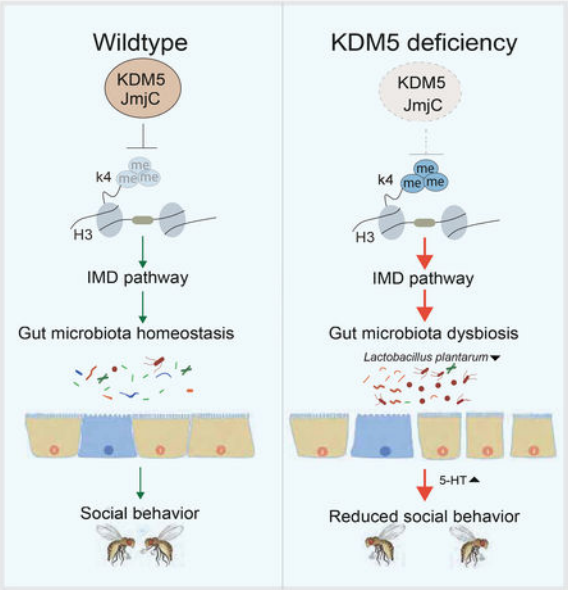

Keywords

KDM5; gut microbiome; demethylase; H3K4me3; behavior

INTRODUCTION

Increasing evidence suggests that the gut microbiota can affect the symptoms of intellectual disability (ID) and autism spectrum disorder (ASD) diseases (Borghi et al., 2017; Caracciolo et al., 2014; Mayer et al., 2014). It is clear that host genes influence the composition of gut microbiota (Wang et al., 2016; Snijders et al., 2016), but the molecular mechanisms that regulate host commensal microbiota homeostasis in normal and disease states remains largely unknown.

Genome-wide association and family studies have identified many genetic contributors to ID and ASD (Shailesh et al., 2016). Loss of function mutations in histone demethylases KDM5A, KDM5B or KDM5C are found in patients with ID and ASD (Fieremans et al., 2015; Martin et al., 2018). KDM5 family proteins are transcriptional regulators that act by demethylating a histone H3K4me3 modification associated with promoters of transcriptional active genes (Secombe et al., 2007). Consistent with the enzymatic activity of KDM5 proteins in the underlying cause of ID and ASD, many missense mutations in KDM5C reduce demethylase enzymatic activity *in vitro* (Brookes et al., 2015). Interestingly, KDM5C functions are highly evolutionarily conserved, as *kdm5c* knockout mice exhibit abnormal learning and social behavior (Iwase et al., 2016; Scandaglia et al., 2017; Martin et al., 2018). A fly strain harboring an allele analogous to a disease-causing missense mutation in human KDM5C ($kdm5^{A512P}$) show learning and memory defects (Zamurrad et al., 2018). Significantly, flies having this mutation show transcriptional and behavioral defects that are indistinguishable from fly strains lacking KDM5 demethylase activity (Zamurrad et al., 2018), further supporting a critical role for the demethylase activity of KDM5 in behavior.

The human genome has four KDM5 paralogs, while the *Drosophila* genome has a single KDM5 ortholog. *Drosophila* is a widely accepted model for studying behavior (Ramdya et al., 2017). In addition, *Drosophila* provides an excellent system in which to study host–microbe interactions because of the ease of its genetic and physiological manipulation, as well as its relatively simple microbial community (Han et al., 2017). Accumulating evidence indicates that the *Drosophila* gut environment is characterized by low bacterial diversity and the most commonly associated bacterial species are members of the *Lactobacillaceae, Enterococcaceae, Acetobacteraceae,* and *Enterobacteraceae* families (Broderick and Lemaitre, 2012; Buchon et al., 2013). These bacteria affect various aspects of *Drosophila* physiology and gut homeostasis including aging (Clark et al., 2015), gene expression (Broderick et al., 2014), metabolic function (Wong et al., 2014) and social behavior (Venu et al., 2014).

Our previous work demonstrated that KDM5 regulates cellular oxidative stress in *Drosophila* (Liu et al., 2014; Liu and Secombe, 2015). It is known that gut epithelial cells contacted by enteric commensal bacteria generate reactive oxygen species in response to microbial signals (Jones and Neish, 2017). In this study, we investigate the mechanistic contribution of KDM5 to social behavior by regulating the gut microbiome composition.

RESULTS

Reduced levels of KDM5 cause intestinal epithelial barrier disruption and impaired social behavior.

To explore the effects of KDM5 on gut homeostasis and social behavior, we generated adult flies with reduced levels of KDM5 using a hypomorphic combination of *kdm5* alleles (*kdm5*$^{K6801/10424}$). *kdm5*$^{K6801/10424}$ flies show dramatically decreased KDM5 protein (Figure 1A) and mRNA expression (Figure 1B) in intestinal tissue, and an accompanying increase in histone H3 lysine 4 trimethylation (H3K4me3).

The intestinal tract of the *kdm5*$^{K6801/10424}$ flies show defects relative to wild-type (*wt*) with bubbles in the midgut (Figures 1C and 1D), which suggested that they maybe gas produced by overgrowth of bacteria. The length of *kdm5* mutant fly midgut is shorter than *wt* while the width is not significantly changed (Figures S1A and S1B). Moreover, electron microscopy showed that the gut of *kdm5*$^{K6801/10424}$ flies displayed a disrupted intestinal epithelial barrier (Figure 1E). A much higher density of bacteria was observed in the gut of *kdm5* mutants as compared to the *wt* (Figure 1E). In the non-absorbable blue food dye experiment, the dye remained within the lumen of the gut of *wt* flies, while it diffused into the abdominal cavity in mutant flies (Figure 1F). In adult flies fed FITC-labeled beads, the beads remained in the lumen of *wt* flies, in contrast, FITC signals were diffuse in the gut epithelial cells of *kdm5*$^{K6801/10424}$ flies (Figure 1G). To avoid confounding our studies with the developmental delay effects of KDM5, we used a temperature sensitive expression system: *Myo1A-Gal4,tub-Gal80*^{TS} to specifically knock-down *kdm5* in the gut of adult flies. Before placing flies at 29°C for 3–7 days to activate *kdm5* knockdown, we reared the flies at 18°C until adulthood. We did not see any developmental defects in the *Myo1A-Gal4*^{TS}/*kdm5*^{RNAi} flies (Figures 1H and S1C–S1E), however these flies showed a shorter life span (Figure S1F) and impaired intestinal barrier integrity and homeostasis compared to control RNAi (Figure 1I). To address whether the defects were caused by differences in food consumption, we assessed the volume of food consumed using a previously described method (Bross et al., 2005). As shown in Figure S1G and S1H, *kdm5*$^{K6801/10424}$ and *Myo1A-Gal4*^{TS}/*kdm5*^{RNAi} flies consumed similar amounts of food compared to *wt* flies. Taken together, these findings indicate that reducing KDM5 in the gut results in more permeable gut tissue.

Alterations in gut–brain axis signaling affect mood and behavior (Nithianantharajah et al., 2017). This led us to test whether reducing KDM5 affects social behavior. Consistent with loss of KDM5 function in ID and ASD patients, *kdm5*$^{K6801/10424}$ adults displayed a significant decrease in social interactions, including social space (Figures 1J and S2A), social avoidance (Figures 1K and S2B) and the total time of direct social contact (Figures 1N for female and S2G for male) compared to *wt* flies. Similar to *kdm5*$^{K6801/10424}$ adults, *Myo1A-Gal4*^{TS}/*kdm5*^{RNAi} flies *at* 29°C showed impaired social behavior (Figures 1L, 1M and 1O for female; Figures S2C, S2D and S2H for male). Importantly, at the non-permissive temperature of 18°C, we do not see any defects in social behavior (Figures S2K–S2M). These data suggest that KDM5 regulates gut homeostasis and influences animal behavior.

KDM5 modulates the microbial composition

Emerging evidence supports the view that gut microbes influence neurochemistry and behavior (Dylan and Bordenstein, 2016). We therefore addressed whether KDM5 affects social behavior by modulating microbiota composition. We performed 16S rRNA gene sequencing using gut DNA isolated from *kdm5*$^{K6801/10424}$ and *wt* flies (Figure S3). The Good's coverage values indicated that the sequencing depth was more than 99.7% (Figure S3A). The gut microbiota of *kdm5*$^{K6801/10424}$ flies had a significantly lower number of observed species compared to *wt* (Figures 2A and 2B). The rarefaction curves result suggested that the lower number of species recovered from *kdm5*$^{K6801/10424}$ animals was not due to insufficient sampling (Figure S3B). A change in the gut microbial community composition was observed in *kdm5*$^{K6801/10424}$ flies compared to *wt* flies (Figure S3C). The gut microbiota of *kdm5*$^{K6801/10424}$ flies showed increased levels of *Proteobacteria* and decreased levels of *Firmicutes* (Figure 2C). Specifically, we found that eight orders were more abundant in the guts of *kdm5*$^{K6801/10424}$ flies relative to *wt*, including gram-negative bacteria, such as *Sphingomonadales, Enterobacteriales* and *Xanthomonadales* (Figure 2D). In contrast, nine orders were less abundant in *kdm5*$^{K6801/10424}$ flies, including those with probiotic properties, such as *Lactobacillales, Bacteroidales* and *Bifidobacteriales* (Figure 2D). In agreement with the gut microbiome sequencing analysis, bacteria culture at 37°C and 25°C revealed that guts from *wt* and flies heterozygous for either of the parental strains (*kdm5*^{k06801} or *kdm5*^{10424}) contained a higher abundance of *Lactobacillus* spp. and lower abundance of gram-negative bacteria than that of *kdm5*$^{K6801/10424}$ (Figures 2E, S3D and S3F). *kdm5*$^{K6801/10424}$ contained higher abundance anaerobic (nutrient agar) and aerobic (mannitol agar) bacteria respectively (Figure S3D). 16S rRNA gene sequencing of these isolated colonies showed decreased of gram-positive *Lactobacillus* spp. and increased of gram-negative bacteria *Providencia* spp. *and Gluconobacter* spp. (Figure S3E). The two species including *Lactobacillus plantarum* L168 (GenBank No. MK049960) and *Providencia rettgeri* P6 (GenBank No. MK049957) were identified by Blast analysis. Changes in abundance of *Lactobacillus plantarum* L168 and *Providencia rettgeri* P6 were independently confirmed by Q-PCR of isolated guts (Figure 2H). *kdm5*$^{K6801/10424}$ flies have an increased ratio of gram-negative bacteria relative to gram-positive bacteria (Figures 2G and S3F). Interestingly, changes in the abundance of *Lactobacillus* spp. and gram-negative bacteria are rescued in transgenic flies expressing HA-tagged KDM5 (Figures 2E and 2F). The gut microbe analysis from *kdm5* RNAi and control RNAi further confirmed that loss of *kdm5* in the intestine shifted the gut microbiota composition as was observed in the *kdm5*$^{K6801/10424}$ (Figures S4A–S4C). Bacterial selective culture assay, gram-staining and PCR further confirmed the analysis (Figures S4D–S4H). Accordingly, at the non-permissive temperature of 18°C, there was no RNAi activation and therefore no decrease in *kdm5* transcript and no increase in IMD/Rel targets (Figure S4I), and importantly, we observed no change in the level of *Lactobacillus* spp. and gram-negative bacteria, as well as the ratio of gram-negative relative to gram-positive bacteria compared to control (Figures S4J–S4M). We conclude that loss of KDM5 in intestine tissue can modulate the microbiome composition.

Intestinal stem cell division rates in *Drosophila* have been used as a marker associated with gut dysbiosis induced by pathogenic-like bacteria overgrowth (Houtz and Buchon, 2014).

Consistent with the microbiome analysis, the number of PH3 positive cells was increased in both *kdm5*$^{K6801/10424}$ and *kdm5* RNAi flies compared to their respective controls (Figures 2I and 2J). However, germ-free (GF) *kdm5* RNAi and GF control RNAi flies showed no significant difference in the number of PH3 positive cells (Figure S5A). GF *kdm5* RNAi flies colonized with microbes from commensal *kdm5* RNAi flies have an increased number of PH3 positive cells relative to GF control RNAi flies colonized with microbes from control RNAi flies (Figure S5B), further linking gut dysbiosis with the observed gut defects.

The nutritional and living environments strongly impact the microbial communities in the gut of flies (Bing et al., 2018). To exclude these effects on the gut microbiota composition, we re-associated *wt* and *kdm5*$^{K6801/10424}$ GF embryos with a microbial community isolated from *wt* flies to colonize both with the same starting microbial input and maintained them in the same culture environment. At one day-old, the total abundance of bacteria levels is very low. Reconstituted GF (R-GF) *kdm5*$^{K6801/10424}$ flies displayed no difference in the number of gram-negative bacteria compared to R-GF *wt* flies (Figure 3A). Gram staining showed no difference in the ratio of gram-negative over positive bacteria in the gut of R-GF *kdm5*$^{K6801/10424}$ and R-GF *wt* flies (Figures 3B and S3G). In contrast, the level of gram-positive *Lactobacillus* spp. increased 5.5-fold in the R-GF *kdm5*$^{K6801/10424}$ flies compared to R-GF *wt* flies (Figure 3C). No significant difference was observed for *P. rettgeri* (Figure 3D). We observed no difference in social behavior between the R-GF *kdm5*$^{K6801/10424}$ and R-GF *wt* flies (Figures 3E–3G). However, at four days of age, R-GF *kdm5*$^{K6801/10424}$ flies displayed a tremendous (15-fold) increase in gram-negative bacteria compared to R-GF *wt* flies (Figures 3H, 3I and S3H). The abundance of *Lactobacillus* was much reduced in R-GF *kdm5*$^{K6801/10424}$ flies (Figure 3J). Q-PCR confirmed decreased levels of *L. plantarum* L168 and increased levels of *P. rettgeri* P6 in R-GF *kdm5*$^{K6801/10424}$ (Figure 3K). Importantly, the R-GF *kdm5*$^{K6801/10424}$ flies showed impaired behavior compared to R-GF *wt* flies (Figures 3L–3N). These observations are consistent with those observed in conventionally cultured *wt* and *kdm5*$^{K6801/10424}$ flies. Furthermore, when we re-associated GF *wt* flies with either *wt* or *kdm5*$^{K6801/10424}$ microbial communities, we observed no changes in the level of *Lactobacillus* (Figure S6A), nor in their behavior (Figures S6B–S6D). Taken together, we conclude that differences in the gut microbiota between the *kdm5*$^{K6801/10424}$ and *wt* flies are due to the reduced levels of KDM5 protein.

Manipulation of gut microbiome rescues KDM5-deficiency induced phenotypes

To more precisely link KDM5's role in the gut microbiome and the observed behavioral phenotypes, we used three approaches to alter the gut microbiome in *kdm5*$^{K6801/10424}$ flies and subsequently quantified their social interactions. We first attempted to generate GF *wt* and *kdm5*$^{K6801/10424}$ flies. Unfortunately, GF *kdm5*$^{K6801/10424}$ flies did not develop beyond the 3rd larval instar stage. However, GF flies with intestinal specific knockdown of KDM5 at the adult of stage were viable. Under GF conditions, KDM5 intestinal specific knockdown and control flies exhibit normal gut epithelia integrity (Figure S5C) and similar social phenotypes (Figure 4A).

Second, antibiotic treatment of conventionally reared *kdm5*$^{K6801/10424}$ flies (Figure 4B) resulted in a significant reduction in stem cell division rates (Figure S7A), intestinal defects

(Figure 4C) and rescued social phenotypes (Figures 4D and 4E for female; S8A and S8B for male). Finally, probiotic treatment of *kdm5*$^{K6801/10424}$ flies with *L. plantarum* L168 (Figure 4F), levels of which were reduced in *kdm5*$^{K6801/10424}$ flies, significantly restored intestinal barrier integrity and reduced the number of intestines with defects in *kdm5*$^{K6801/10424}$ flies (Figures 4G and 4H). Additionally, we observed that probiotic-treated *kdm5*$^{K6801/10424}$ flies had significantly increased social interactions, including social space and social avoidance (Figures 4I and 4J for female; S8C and S8D for male). Moreover, probiotic treatment with *L. plantarum* L168 or antibiotic treatment of flies with intestinal specific KDM5 knockdown significantly improved social interaction (Figures 4K–4N and S8G for female; S8E, S8F and S8H for male). Similar treatment of *wt* flies using antibiotics or *L. plantarum* L168 did not show social avoidance and social space differences in behavior (Figures S8I–S8K). These results indicate that reduced KDM5 causes a change in social behavior at least partially through altering the gut microbiome.

Our previous studies showed that levels of tryptophan, an essential serotonin precursor linked to hyperserotonemia and ASD, were increased in *kdm5*$^{K6801/10424}$ flies (Liu and Secombe, 2015). We therefore assessed the serotonin (5-HT) concentration in *wt* and *kdm5*$^{K6801/10424}$ flies. Similar to the findings in ASD patients (Chen et al., 2017), we observed that the abdomens and gut *kdm5*$^{K6801/10424}$ flies had significantly higher levels of 5-HT compared to *wt* flies (Figures 4O and S8L). Interestingly, heads and guts of flies with intestine specific KDM5 knockdown also showed elevated levels of 5-HT (Figures 4R and S8M). Not surprisingly, *kdm5*$^{K6801/10424}$ and intestine specific KDM5 knockdown flies treated with *L. plantarum* L168 or antibiotics showed a significant decrease in 5-HT levels (Figures 4P, 4Q and 4S). Our results are consistent with evidence that manipulating the microbial composition of the gastrointestinal tract can modulate plasma concentrations of neurotransmitters (Clarke et al., 2014).

Lifespan is very important for considering both behavioral and gut phenotypes. Our previous studies reported that hypomorphic *kdm5*$^{k6801/10424}$ have a shorter lifespan compared to *wt* flies (Liu et al., 2014), so we investigated whether antibiotic treatment or supplementing with *L. plantarum* can extend the survival of *kdm5*$^{k6801/10424}$ mutants. GF *kdm5*$^{k6801/10424}$ flies supplemented with *L. plantarum* at embryogenesis are rescued resulting in a 3.5-fold increase in median survival (28 days) compared to conventionally reared *kdm5* mutant flies (8 days) (Figure S8O). Moreover, conventionally reared *kdm5* mutant flies treated with antibiotics show a 2.3-fold increase in median life span from eight to 19 days (Figure S8P), indicating that the developmental defects of *kdm5* mutants can be partially rescued by modulating the gut microbiota either by feeding them with probiotic *L. plantarum* or by treating them with antibiotics.

KDM5 negatively regulates IMD/Rel signaling

To identify the molecular mechanism by which KDM5 shapes the gut microbiome, we performed RNA-seq analysis of intestines from *wt* and *kdm5*$^{K6801/10424}$ flies. We identified 1761 transcripts that were significantly differentially expressed between *kdm5*$^{K6801/10424}$ and *wt* flies (Figure 5A). Analyses of KDM5-regulated genes revealed enrichment for a number of diverse biological processes (GO categories), including innate immune response

pathway and defense bacterial infection (Figure 5B). Gene network analysis showed a critical role of KDM5 in the activation of genes required for the immune deficiency (IMD) pathway (Figure 5C). Recent research indicates that the innate immune system plays an important role in shaping the microbiota community into configurations that can be tolerated by the host and are beneficial for its metabolic activities (Thaiss et al., 2016). We therefore investigated whether KDM5 has a direct role in maintaining gut microbiota homeostasis by regulating genes required for the innate immune response. Up-regulation of IMD pathway genes in intestinal tissue of *kdm5*$^{K6801/10424}$ flies was further confirmed by real-time PCR (Figure 5D). It is possible that activation of IMD pathway could be mediated by the altered microbiota in *kdm5*$^{K6801/10424}$ rather than through direct KDM5-mediated changes to gene expression *in vivo*. To test this, we knocked down *kdm5* expression *ex vivo* using cultured S2 cells and assessed IMD pathway genes expression. Knockdown of *kdm5* resulted in moderate activation of IMD pathway targeted genes in S2 cells compared to positive control S2 cells treated with IMD pathway regulators 20-hydroxyecdysone (20E) or peptidoglycan (PGN) (Figures S9C–S9E and S9G–S9I). Moreover, knockdown of *kdm5* activated *imd* expression whereas 20E nor PGN treatment did not (Figure S9A). Consistent with these results, GF *kdm5* RNAi also showed elevated expression of *immune deficiency (imd), Diptericin A (DptA), Attacin-B (AttB)* and the RE isoform of Peptidoglycan Recognition Protein *LC (PGRP-LC-RE)* (Figure S5D). Together these data show that KDM5 is involved in activation of the IMD pathway.

In agreement with the observation that antibiotic and *L. plantarum* L168 partially rescued the intestinal permeability of *kdm5*$^{K6801/10424}$ (Figure 4G), we observed reduced the expression of IMD pathway target genes (Figure 5E). While the gram-positive bacterium *L. plantarum* has a gram-negative type (DAP-type) peptidoglycan, that induces IMD (Asong et al., 2009), it is not obvious why *L. plantarum* L168 reduces *imd* and alters IMD signaling. We investigated whether treatment with *L. plantarum* shifted the gut microbiota composition of *kdm5*$^{K6801/10424}$ flies. We indeed found that *L. plantarum* treatment increased the species diversity of *kdm5*$^{K6801/10424}$ flies (Figure S10A) and changed their gut microbiota composition (Figures S10B and S10C). Similar to the gut microbiome of *wt*, the *kdm5*$^{K6801/10424}$ with *L. plantarum* treatment showed decrease of *Acetobacter* and *Gluconobacter* compared to *kdm5*$^{K6801/10424}$ (Figures S10C and S3E). Moreover, the gut microbiome composition in the *kdm5* mutants with *L. plantarum* treatment is similar to that in *wt* (Figure S10D). The result suggested *L. plantarum* restore partially gut microbiota homeostasis. Thus, loss of KDM5 results in activation of IMD signaling, and KDM5 induced dysbiosis leads to further activation of IMD, which can be balanced by treatment with *L. plantarum L168*.

IMD, *PGRP-LC* and *PGRP-LE* play central roles in bacterial recognition, resolution and induction of the IMD/Rel pathway (Bosco-Drayon et al., 2012; Choe et al., 2002; Neyen et al., 2016). Through alternative splicing the *PGRP-LC* gene has the potential to generate eight *PGRP-LC* isoforms. To investigate whether KDM5 regulates the relative abundance of specific *PGRP-LC* isoforms, we examined *PGRP-LC* isoforms mRNA level and found significantly increased expression of the *PGRP-LC-RE* transcript in KDM5 deficient cells and intestine tissue (Figures S11A and S11B), whereas other *PGRP-LC* isoforms and *PGRP-LE* had no significant change relative to *wt* (Figures S11A and S11C). To address whether

PGRP-LC-RE and *imd* can activate the IMD pathway, we over-expressed both *PGRP-LC-RE* and *imd* in S2 cells and found that co-overexpression of *imd* and *PGRP-LC-RE* enhanced slightly Relish target gene expression compared to the group with overexpression of *PGRP-LC-RE* or *imd* alone (Figure S11D). These data suggest that the protein encoded by *PGRP-LC-RE* may act as a co-factor with *imd* to regulate the IMD pathway.

Differential exon incorporation analysis revealed that an increase in expression of the *PGRP-LC-RE* isoform in KDM5 deficient cells is due to altered splicing (Figure 5F). Publicly available KDM5 (GEO: GSE70591) and H3K4me3 (GEO: GSM400670) chromatin immunoprecipitation sequencing (ChIP-seq) data show that KDM5 and H3K4me3 are enriched at the transcription start sites (TSSs) of *imd* and *PGRP-LC* (Figures S11E–S11H), which were confirmed by ChIP-PCR (Figures 5G and 5H). *PGRP-LC* has two enrichment peaks of KDM5 and H3K4me3 involved in different isoforms transcription including *PGRP-LC-RA* and *PGRP-LC-RE* (Figures S11E and S11F). It has been suggested that histone modification information, such as H3K4me3, is predictive of mRNA production (Chen et al., 2015). We found a significant increase in levels of H3K4me3 in the *PGRP-LC-RE* promoter regions in $kdm5^{K6801/10424}$ flies relative to *wt* (Figure 5H, right panel) and an accompanying increase in full-length *PGRP-LC-RE* expression levels in intestinal tissues of $kdm5^{K6801/10424}$ flies, KDM5 intestine-specific RNAi flies and $KDM5^{RNAi}$ S2 cells compared to *wt flies*, Control flies and GFP^{RNAi} S2 cells respectively (Figure 5I). In contrast, *PGRP-LC-RA* has no change to promoter proximal H3K4me3 in $kdm5^{K6801/10424}$ flies relative to *wt* (Figure 5H, right panel) and full-length mRNA levels (Figure 5I). These data suggest that the histone demethylase activity of KDM5 is involved in the regulation of activation of IMD/Rel pathway by repressing *imd* expression and exon splicing of *PGRP-LC*.

Relish is the *Drosophila* NF-kappaB that is primarily associated with and activated by the IMD signaling response to gram negative bacterial infection (Hetru and Hoffmann, 2009). Consistent with IMD/Rel activation, the majority of Relish trans-localized into the nucleus in intestinal tissue of $kdm5^{K6801/10424}$ flies (Figure 5J). In agreement with this observation, reducing KDM5 increased Relish recruitment at promoter regions of target genes including *AttA, AttC, AttD, Dro* and *Mtk* (Figure 5K). Significantly however, we did not observe KDM5 and H3K4me3 enrichment at the promoter regions of Relish direct target genes (Figures S11I and S11J). These data suggest that KDM5 may indirectly repress Relish complexes by affecting its binding to target genes promoters through regulating component genes of IMD pathway.

KDM5 demethylase activity regulates IMD/Rel pathway activity and gut-microbiome-brain function

Recent studies emphasize the importance of KDM5 demethylase in neuro developmental disorders (Wei et al., 2016; Zamurrad et al., 2018). We propose that the demethylase activity of KDM5 may be particularly relevant to our understanding of the link between gut microbiota and social behavior. To test whether KDM5 activation of the IMD pathway is dependent on its demethylase activity, we examined gene expression levels in the intestine tissues of flies specifically lacking enzymatic activity in the hypomorphic mutant

kdm5$^{k6801/k6801}$ background (Navarro-Costa et al., 2016). Of the ten genes related to innate immune pathway function tested, all were up-regulated in *kdm5*^{JmjC*} flies similar to that of *kdm5*$^{K6801/10424}$ flies (Figure 6A). Consistent with data from *kdm5*$^{K6801/10424}$ flies, Relish protein was enriched in the nuclei of intestinal tissue in *kdm5*^{JmjC*} flies (Figures S11K). Furthermore, we found a significant increase in levels of H3K4me3 at the promoters of the *PGRP-LC-RE* and *imd* genes in *kdm5*^{JmjC*} flies relative to that of *wt*, but not in the promoter region of *PGRP-LC-RA* (Figure S11L). Similar to *kdm5*$^{K6801/10424}$ flies, Relish binding to five of its target genes was increased in the intestine of *kdm5*^{JmjC*} flies (Figure S11M). These data identified a function for the JmjC domain-encoded enzymatic activity of KDM5 in innate immune signaling.

To determine the role of the demethylase activity of KDM5 in modulation of the gut-microbiome-brain axis, we measured the *Lactobacillus* spp. abundance and social behavior of KDM5 demethylase inactivated flies. Similar to *kdm5*$^{K6801/10424}$ flies, KDM5 demethylase inactivated flies showed a significant reduction of *Lactobacillus* spp. and increase of gram-negative bacteria, *Providencia rettgeri* (Figures 6B and 6C), and an increase in the number of PH3 positive cells (Figure 6D). Also, antibiotic treatment of conventional *kdm5*^{JmjC*} flies resulted in a significant reduction in stem cell division rates (Figure S7B). Consistent with a role for the demethylase activity of KDM5 in maintaining gut microbiome homeostasis, we found that *kdm5*^{JmjC*} flies displayed impaired intestinal integrity and gut epithelium permeability (Figures 6E and 6F). Accordingly, KDM5 demethylase inactivated flies showed defective social behavior and increased 5-HT level (Figures 6G, 6H, 6L, S2E, S2F, S2I, S2J and S8N). Probiotic treatment of *kdm5*^{JmjC*} flies with *L. plantarum* L168 reduced intestinal permeability (Figure 6I), rescued the defective social interaction activity and decreased 5-HT level (Figures 6J, 6K and 6M). Taken together, these results indicate that KDM5 modulates social behavior and maintains gut microbiota homeostasis dependent on its demethylase enzyme activity.

Inhibition of IMD signaling rescues gut dysbiosis and social interaction behavior induced by loss of KDM5

Since down-regulation of KDM5 elevates IMD pathway activity (Figure 5), we asked whether inhibition of IMD signaling can rescue gut dysbiosis and the social interaction phenotype of KDM5 gut knockdown flies. As shown in the Figure S12A, flies with down-regulation of both *imd* and *kdm5* in intestinal tissue showed down-regulation of IMD/Rel signaling target gene expression compared to flies with knock-down of *kdm5* alone. Consistent with q-PCR data, we also observed that knockdown of both *imd* and *kdm5* decreased the abundance of Gram-negative bacteria, *Providencia rettgeri*, and increased *L. plantarum* relative to KDM5 RNAi flies alone (Figures 7A, 7B and S12B). Also, the double knockdown flies rescued the increased gut permeability phenotype (Figure 7C), improved social space and social contacting time (Figures 7D–7F) and the decreased serotonin production (Figure 7G) compared to *kdm5* RNAi group alone. In addition, we found no change in the expression of *kdm5* in the gut of *imd* gut-specific knockdown flies (Figure S12A), suggesting that the rescued phenotype was the result of IMD pathway regulation by KDM5 and not KDM5 regulation by IMD.

DISCUSSION

In this study, we discovered a role of the histone demethylase KDM5 in maintaining gut innate immune, bacteria and metabolic homeostasis by regulation of IMD signaling, and subsequently social behavior through the gut-microbiome-brain axis partially.

In flies, chronic over-activation of the IMD pathway in the gut leads to the secretion of antimicrobial peptides (AMPs) and causes dysbiosis ultimately resulting in death (Lee and Lee, 2014). We observed overgrowth of pathogenic-like bacteria and a decrease of commensal bacteria in KDM5 deficient flies, in agreement with previous research that maintenance of innate immune homeostasis is associated with suppression of pathogenic bacteria (Han et al., 2017). Moreover, these results support that the KDM5 demethylase has a direct role in maintaining gut microbiota homeostasis by regulating genes required for innate immune response, which sustain the concept that *Drosophila* have evolved a rich array of regulatory mechanisms to safeguard homeostatic IMD signaling (Buchon et al., 2013). Moreover, KDM5B is required for innate immune responses in mammalian cells (Ptaschinski et al., 2015). Given the evolutionary conservation of the IMD/Rel pathway, it will be important to evaluate whether mammalian KDM5A/B/C regulates gut microbiota homeostasis to affect animal behavior through modulating innate immune response. We noticed that microbial manipulation cannot rescue social behavior of KDM5 deficient flies completely, which implies that KDM5 may also affect social behavior through other pathways.

In our study, we found that loss of KDM5's demethylase activity led to an increase in H3K4me3 levels at sites upstream of the TSS of *imd* and altered splicing efficiency of the *PGRP-LC-RE* isoform, which resulted in aberrant activation of IMD signaling *in vivo*. Neyen et al., showed that overexpression of *PGRP-LC-RE* in the fat body reduced the immune response to polymeric PGN of dead bacteria (Neyen et al., 2016). The exact mechanism of *PGRP-LC-RE* mediated activation of the IMD pathway in the gut remains to be clarified. FOXO-dependent regulation of innate immune homeostasis has been reported (Becker et al., 2010), and our previous study showed that KDM5 interacts with FOXO to regulate cellular oxidative stress (Liu et al., 2014). Further investigations will need to clarify the potential role of FOXO signaling in KDM5 regulated maintenance of host-commensal bacteria homeostasis.

Acetobacter and *Lactobacillus* are digestive symbionts in the fly digestive system with important roles in animal development and physiology (Broderick et al., 2014). In our study, we found significantly decreased abundance of *Lactobacillus* in $kdm5^{K6801/10424}$ flies. Our study focused on *L. plantarum*, but it is likely that other *Lactobacillus* species can also rescue the development defects of $kdm5^{K6801/10424}$ flies. In addition, bacteria of the genus *Acetobacter* are present at increased abundance in the gut of $kdm5^{K6801/10424}$ flies. The exact role of other *Lactobacillus* and *Acetobacter* species in the development of $kdm5^{K6801/10424}$ flies needs to be tested in future studies. Recently, Broderick et al. (2014) provided evidence that the microbiota has robust and consistent effects on gut physiology, as measured by gene expression, which implicated that *L. plantarum* may influence host gene

expression in GF *kdm5*$^{K6801/10424}$ flies to exert its impact on larval development adult survival, gut phenotypes and behavior.

Increasing research has emphasized the role of IMD in guiding the conversation between bacteria and host, which may act as a central regulator to integrate host defense, the physiology and animal behavior of the whole organism (Zhai et al., 2018). The landscape of protein-protein interactions in *Drosophila* IMD signaling has recently been revealed by the Hoffmann group (Fukuyama et al., 2013). Impressively, we noted that many of the protein interactions with IMD signaling have previously been found to be associated with ASD, suggesting that ASD may at least partly be affected aberrant IMD signaling, further leading to gut dysbiosis and abnormal behavior.

In summary, our results support the model that the histone demethylase KDM5 is a critical host transcriptional regulator that maintains immune homeostasis and is responsible for preservation of the normal commensal microbial community structure and behavior. Neurodevelopmental disorders like ID and ASD present an enormous challenge to affected individuals, their families and society (Koemans et al., 2017). Our research suggests that direct modification of the gut microbiome can serve as clinical therapeutic approach for ID and ASD patients with aberrant IMD signaling.

STARMETHODS

CONTACT FOR REAGENT AND RESOURCE SHARING

Further information and reagent requests may be directed to the Lead Contact Xingyin Liu (xingyinliu@njmu.edu.cn).

EXPERIMENTAL MODEL AND SUBJECT DETAILS

Fly Husbandry and Fly stocks—The standard medium for rearing *Drosophila* is as described previously (Qian et al., 2017). Briefly, for 12 L of medium, 252.966 g sucrose (Sinopharm Chemical Reagent Co., Ltd, cat. #10021418), 505.92 g glucose (Sinopharm Chemical Reagent Co., Ltd, cat. #63005518), 249.52 g yeast powder (Angel) were dissolved in 4 L of 100°C water; 84.8 g agar (BioFroxx, cat. #1182GR500) and 2.5 L water were added; 621.6 g cornmeal flour and 7 L water were added; after which 5.808 g $CaCl_2$ was added (Sinopharm Chemical Reagent Co.,Ltd, cat. #10005860), incubated for 15 min at 100°C; 16 g of potassium sorbate (Aladdin, cat. #P103845) was added after 15 min thermal insulation. Antibiotic media was prepared by adding 1 mL of a 100× stock of antibiotics per 100 mL of liquefied food to a final concentration of 100 μg/mL Ampicillin, 50 μg/mL Kanamycin, 50 μg/mL Tetracyclin and 200 μg/mL Rifamycin to remove over-growth of pathogenic-like bacteria.

Fly stocks were maintained at 25°C on standard media, 50–60% humidity, and 12 hour light/dark cycle. The *w*^{1118}, *kdm5*^{10424}, *kdm5*^{K06801}, KDM5-RNAi (TRIP line 28944), IMD-RNAi (TRIP line 38933) were obtained from the Bloomington stock center. The demethylase-inactive (*kdm5*^{JmjC*}) fly strain was reported previously (Navarrocosta et al., 2016). *kdm5*^{JmjC*} transgenes were subsequently crossed into the *kdm5*$^{k6801/+}$ mutant background. The *kdm5*^{k6801}*;gkdm5-HA* fly strain was reported previously (Liu and

Secombe, 2015). The stock, Myo1A-Gal4^{TS},UAS:GFP,tubulin-Gal80^{TS} was from Julie Secombe Lab.

S2 Cell Line—Male S2 cell (ATCC CRL-1963) were cultured in Schneider's drosophila media (Gibco, Cat#21720–024), 90%; heat-inactivated fetal bovine serum (Gibco, Cat#10099141), 10%, supplemented with 50 U/ml Penicillin G, 50 μg/ml Streptomycin sulfate(Gibco, Cat# 15140122). S2 cells were grown at 25°C without CO2 as a loose, semi-adherent monolayer in tissue culture flasks or plates.

METHOD DETAILS

KDM5 and/ or IMD knockdown in intestine tissue at the adult stage—We avoided confounding our studies with the developmental effects of KDM5 by using the temperature sensitive gal4: Myo1A-Gal4^{TS},tub-gal80^{TS} to specifically knock-down *kdm5* and/or *imd* in adults. Before activating *kdm5* and/or *imd* knockdown, we reared the flies at 18°C until adulthood, then transferred flies at 29°C for 3–7 days to induce down-regulation of KDM5 and/or IMD.

Germ-free flies and re-colonization of Germ-free flies—Germ-free flies were generated following the previous report with minor modification (Ryu et al., 2008). After crossing the flies, resulting embryonic progeny were washed with 2.7% sodium hypochlorite, 70% ethanol, 0.1% Triton X-100 and sterile water. The embryos were placed, and larvae maintained on axenic food until adult stage. Once the flies reached adulthood, total DNA was isolated from a selection of flies to confirm absence of bacterial contamination by performing culturing tissues on LB plates and 16S rRNA gene PCR analysis. GF flies were re-colonized by incubating axenic lines with bacterial isolated from the guts of conventionally reared flies. The gut bacteria were isolated by dissecting 5 guts in 200 μL PBS, vortexed, spin down, and then resuspended in 200 μL of 1× PBS. Bacteria cell counts were determined with Neubauer-improved counting chamber (Paul Marienfeld GmbH & Co.KG, German). 100 μL bacterial suspensions with 1 ×10^{6} cells were transferred to the surface of germ-free *Drosophila* food for 30min. Then germ-free eggs or adults were reared on this food. For *L. plantarum reassociation* as previously described (Broderick et al., 2014). *L. plantarum* were grown overnight in 20 mL of MRS medium in a incubator at 37°C. Cultures were spin down for 20 min at 4,000 r pm at 4°C, and the pellet was rinsed two times and then resuspended in 5 ml of 1× PBS. Each culture was adjusted to a concentration of 1×10^{7} CFU/mL. The isolated gut bacteria and *L. plantarum* culture was allowed to soak into the medium for 30 min before either axenic embryos or flies were added.

16S rRNA sequencing and analysis—Gut DNA was prepared from 20 dissected intestinal tissue from female (3–7 days old) w^{1118}, $kdm5^{10424/k6801}$, $kdm5^{10424/k6801}$, $kdm5^{10424/k6801}$ with *L. plantarum* treatment, *Myo1A-Gal4^{TS}/+* and *Myo1A-Gal4^{TS}/kdm5 RNAi* respectively using fecal DNA extacting kit (Tiangen Company, Beijing, China). 3 to 5 biological replicates per group were performed. DNA quality was monitored on 1% agarose gels. For w^{1118} and $kdm5^{10424/k6801}$, $kdm5^{10424/k6801}$ *and* $kdm5^{10424/k6801}$ with *L. plantuarum* treatment, the V4 regions of 16S rRNA genes were amplified using barcoded

primers. The 16S rRNA V4 specific primers are 515F (5'-GTGCCAGCMGCCGCGGTAA-3') and 806A (5'-GGACTACHVGGGTWTCTAAT-3'). For Myo1A-Gal4$^{TS/+}$ and Myo1A-Gal4^{TS}/*kdm5 RNAi*, the V3–V4 hypervariable regions of the bacteria 16S rRNA gene were amplified with primers 338F (5'-ACTCCTACGGGAGGCAGCAG-3') and 806R (5'-GGACTACHVGGGTWTCTAAT-3'). PCR reactions were carried out in 30 μL reactions with 15 μL of Phusion® High-Fidelity PCR Master Mix (New England Biolabs), 0.2 μM of forward and reverse primers, and 10 ng template DNA. Thermal cycling consisted of initial denaturation at 98°C for 1 min, followed by 30 cycles of denaturation at 98°C for 10 s, annealing at 50°C for 30 s, and elongation at 72°C for 30 s. Finally, 72°C for 5 min. PCR products were detected on 2% agarose gels by electrophoresis. PCR products were purified using the GeneJET Gel Extraction Kit (Thermo Scientific). Sequencing libraries were generated using Illumina TruSeq DNA PCR-Free Library Preparation Kit (Illumina, USA) following manufacturer's recommendations and index codes were added. The sequence were performed by Illumina Hiseq platorm (NovoGene Co. Ltd and Biomarker Co. Ltd respectively). Sequences were analyzed using QIIME software package 1.9 (Caporaso et al., 2010), and in-house Perl scripts were used to analyze alpha- (within samples) and beta-(among samples) diversity. QIIME calculates both weighted and unweighted unifrac, which are phylogenetic measures of beta diversity. We used unweighted unifrac for Principal Coordinate Analysis (PCoA) and Unweighted Pair Group Method waith Arithmetic mean (UPGMA) Clustering. To eliminate potential contaminants in kit components or water, only OTUs with an average relative abundance $\geq 10^{-4}$ and found in at least 10% of the subjects were considered for analyses. All 16s rRNA datasets are publically available (NCBI GEO accession numbers: GSE98944, GSE98945).

Quantification of bacterial species by q-PCR—Gut DNA extraction from 3–7 days old females flies were performed as described above for amplicon sequencing. DNA was isolated from pools of ten guts each. 0.5 ng DNA was used for the q-PCR template. The q-PCR reactions were conducted in two independent biological replicates using Quant Studio5 (Applied biosystems) and SYBR Green PCR master mix (Vazyme). The *Drosophila* GAPDH gene was used for normalization and $2^{-\Delta CT}$ values were plotted as previously described (Sebald et al., 2016). PCR primers for detection of specific bacterial species are shown in Table S1.

RNA extraction, cDNA library preparation, RNA-Seq sequencing—Total RNA was extracted from two separate samples of 30 dissected digestive tracts from 3–5 day old female w^{1118} and $kdm5^{10424/k6801}$ adult flies using TRIZOL (Life science) and the DNA-free kit (Ambion). RNA concentrations were quantified using a NanoDrop Spectrophotometer and sample integrity was verified using an Agilent 2100 Bioanalyzer (Agilent Technologies Inc). Only samples with RIN values above 8.0 were used for experiments. cDNA libraries were prepared using an Illumina TruSeq RNA sample prep kit. The average size of the library cDNAs was 150 bp (excluding adapters). The integrity and quality of cDNA libraries were assessed using an Agilent 2100 Bioanalyzer and an ABI StepOne Plus real-time PCR system. RNA-seq was performed by Novogene Company (Tianjin, China). RNA-Seq reads from the FASTQ files were mapped to the *Drosophila* reference genome (R6.23) using Tophat2 (Kim et al., 2013). The output files in BAM

(binary alignment/map) format were analyzed by Cufflinks to estimate the transcript abundance and the presence of putative mRNA isoforms. The transcript expression level was calculated using TPM (Transcripts Per Kilobase Million). Exon splicing analysis was performed using the DExSeq Bioconductor package by controlling for false discovery rate (FDR) at 0.1(10%) (Anders et al., 2012). The accession number for the RNA-Seq data is GEO GSE98943.

Bacterial culture and colonies analysis—four female flies from each genotype were sterilized in 95% ethanol for 1 min and dissected their guts, and then the guts were placed in 200ul of 1×PBS in a 1.5-ml screw-top microcentrifuge tube containing glass beads. Samples were homogenized using a muti-tissue sample crusher (Shanghai Jingxin Industrial developmental company, China) for 60 s, or cut gut into small pieces and vortex them for 30 s, then spin down 30 s at 1000 rpm and take out supernatants. The five 1/10 dilutions for the supernatants were made and plated on mannitol-agar plates or nutrient-agar plates following previously published methods (Broderick et al., 2014). The aerobes were cultured on mannitol-agar plates at 25°C for 48–96 hr, the anaerobes were cultured on nutrient-agar plates at 25°C under strict anaerobic conditions for 48–96 hr. Another group of 1/10 dilution were plated on MRS plates at 37°C for 24 hr and 25°C 48–96 hr. To compare the abundance of gram-negative bacteria in the gut of flies with different genotypes, gram-negative bacteria selective medium was used to selectively culture gram-negative bacteria. One liter of gram-negative bacteria selective medium contains 5 g Trypsin, 2 g Yeast extract powder, 2 mg crystal violet, 1 g Non-fat milk powder, 1.6 mg Nisin and 15 g agar. After sterilization at 121°C for 15 minutes, the media is cooled to 45–50°C, before adding 90-unit p enicillin G for each 200 mL aliquot of medium.

Colony analysis was performed as previously described (Broderick et al., 2014). First, bacterial colonies on mannitol-agar plates were identified based on classic morphological features (color, shape, margins, elevation, and texture), and then two isolates from each designated morphology were purified to obtain individual colonies. A total of 37 representative colonies from *wt* gut and 40 representative colonies from $kdm5^{10424/k6801}$ were identified by 16S rRNA gene PCR with using primers 27F (5'-AGAGTTTGATCCTCMTGGCTCAG-3') and 1492R (5'-GATTACCTTGTTACGACTT-3'). 16S rRNA gene sequence data was characterized by BLAST analysis, and then species with the highest similarity were deduced as genus name of the unknown colonies. Relative frequency of bacterial 16S rRNA clones from two groups was counted. All of sequences data were submitted to GenBank under accession numbers MK049952, MK049953, MK049954, MK049955, MK049956, MK049957, MK049958, MK049959, MK049960 and MK049961.

Assessment of consumed food volumes—To address whether $kdm5^{10424/k6801}$ and $Myo1A\text{-}gal4^{TS}/kdm5^{RNAi}$ knockdown flies ingest different amounts of food compared to control flies, we assessed consumed food volumes as previously described (Bross et al., 2005). 8–12 female flies at the age of 3–7 days old each group were fasted for 1 hr before testing and transferred to 1% blue dye food for 6 hr. After that, fly heads were separated and the bodies were transferred to a 1.5 mL tube with 0.4 mL PBS, ground completely and

centrifuged at 13000 rpm for 25 min. The supernatant was transferred to a new 1.5 mL tube and centrifuged at 13000 rpm for 25 min, after which the supernatant was collected for testing. A standard curve was established by dissolving blue dye with PBS to a concentration of 0.1%. 0, 10, 20, 40, 60, 80, 100 μL stock solutions were diluted to 1.5 mL. The absorbance of samples and standard solution were then measured at 625 nm (BioTek Synergy HIGHLAND PARK, ROX 998). At lease two independent biological replicates each group were performed.

Intestine integrity analysis—Integrity of intestinal barrier function was assessed by measuring the post-feeding distribution of a non-absorbable blue food dye (Solarbio cat#E8501) according to the published method (Wu et al., 2017). 10–20 female flies at the age of 3–7 days each group were transferred from normal food to blue dye food (2.5% w/v) for 6–10 hr. The gut integrity was determined by quantifying the blue dye coloration seen in the body cavity using ImageJ. At lease two independent biological replicates each group were performed.

Feeding assay with FITC-labeled beads—3–7 days old female flies were starved for 3 hr at 25°C before feeding FITC-labeled beads (30 nm diameter, Polysciences, Warrington, PA, USA) to monitor the permeability of the anterior midgut, as described previously (Kenmoku et al., 2016). The guts were dissected after feeding for 15–30 min, and then put guts on the slides and captured image using an Olympus conventional fluorescence microscope. 10 to 15 female flies each group were performed the assay. The fluorescence density was quantified using Image J. Statistical significance was evaluated using t-test of GraphPad Prism 6.0. At lease two independent biological replicates each group were performed.

Chromatin immunoprecipitation—ChIP was performed using 300 digestive tracts from 3–7 days old female flies as previously described (Liu et al., 2014). Cross-linking was performed for 15 min using 1.8% formaldehyde during tissue homogenization. Chromatin extracts were sonicated using a sonicater (Biosafer, China) for 30 min (settings 10 s on, 10 s off, high power) to give rise to sheared chromatin with an average length of 200 to 800 bp. Immunoprecipitations were performed using 2–4 μg of anti-Relish, anti-KDM5 and anti-H3K4me3 for ChIP-qPCR. IgG was used as a negative control. Triplicates from two independent biological replicates were analyzed following the ΔCt method. Data are expressed as the percentage of input chromatin precipitated for each region examined. Table S1 lists all of ChIP-qPCR primers.

Functional interpretation of deferentially expressed genes and gene network analysis—Degree of enrichment for cellular component, biological processes and molecular functions was assessed using the Gene ontology (GO) program DAVID (Huang et al., 2009). Protein-protein integration data are retrieved from the STRING Database (http://string-db.org/), and protein–protein interaction networks are visualized using Cytoscape version 3.4.0. Colors of the nodes indicated the expression changes.

Immunofluorescence—The digestive tracts of 3–7 days old female *wt*, $kdm5^{10424/K6801}$ and $kdm5^{JmjC*}$ flies were dissected in 1×PBS respectively. Immunofluorescence was carried

out as described (Wu et al., 2017). Whole guts were fixed in 1×PBS with 4% paraformaldehyde for 30 min at 25°C. Samples were washed in PBS with 0.1% T riton X-100 (PBST) three times, 10 min each. Then the tissues were prewashed in 5% BSA in PBST for at least 30 min at 25°C. For anti-PH3 antibody staining, the samples were fixed with 3.7% formaldehyde in PBS, permeabilized with 99.5% pre-chilled ethanol at −30°C for 5 min per the previous published method (Kenmoku et al., 2016). Samples were incubated with anti-Relish (RayBiotech) or anti-PH3 (Cell signaling) at 1:100 dilution overnight. After washing three times 10 min each in PBST, samples were incubated with secondary antibody (1:500) for 1–2 h at 25°C. DNA was visualized with DAPI Fluoromount-GTM (YEASON). Images were acquired using a FluoView FL1200 laser scanning confocal microscope (Olympus).

L. plantarum* identification and feeding—L. plantarum* L168 was isolated from gut of 3–4 days old female *wt* flies digestive tracts using MRS (peptone 10 g/L, beef extract 10 g/L, yeast 5 g/L, glucose 5 g/L, sodium acetate trihydrate 5 g/L, Ammonium citrate dibasic 2 g/L, tween 80 1 g/L, K_2HPO_4 2 g/L, $MgSO_4$·7H2O 0.2 g/L, $MnSO_4$·H_2O 0.05 g/L, $CaCO_3$ 20 g/L, agar 15 g/L) medium at 37°C under anaerobic conditions. Six colonies were cultured in MRS liquid medium at 37°C overnight. Genomic DNA was extracted and 16S rRNA was amplified using primers Lac-F (5'-gaatgtgtactgccataact-3') and Lac-R (5'-gcaactgcatagtattgtgc-3'). The products indicated the colonies are most likely *L. plantarum*. Next, to confirm whether the strain is *L. plantarum*, we cloned the bsh gene of *L. plantarum* using *bsh* specific primers, bsh-F (5'-atgtgtactgccataactta-3') and bsh-R (5'-ttagttaactgcatagtattg-3'). We also tested for *L. plantarum* specific physiological and biochemical characteristics (cat. #shbg13, Haibo Company, China). Since *Lactobacillus* is resistant to vancomycin (Tynkkynen et al., 1998), to abolish other pathogenic bacteria, newborn $kdm5^{K6801/10424}$, $KDM5^{RNAi}$ and $kdm5^{Jmjc*}$ mutant flies were transferred to a diet containing vancomycin (30 μg/mL) 1–2 days before feeding *L. plantarum* L168 or normal food. Social behavior analysis was performed on flies after feeding with *L. plantarum* L168 or normal food for 2–3 days. *L. plantarum* L168 culture was prepared fresh every day.

Providencia rettgeri* identification—Providencia rettgeri* bacteria were isolated from 3–4 days old female $kdm5^{K6801/10424}$ flie digestive tracts by culturing on mannitol-agar plates at 37°C for 24 hr. Genomic DNA was extracted and 16S rRNA gene was amplified using primers 27F (5'-AGAGTTTGATCMTGGCTCAG-3') and 1492R (5'-GATTACCTTGTTACGACTT-3'). A total of 86 colonies were sequenced. The sequencing results showed that some of the colonies shared 100% homology with *Providencia rettgeri* through BLAST searching.

Social space analysis—The social space assay has been used to quantify social interactions of *D. melanogaster* or other small insects (Mcneil et al., 2015). One to two days prior to the experiment, 15 to 20 (3–7 days old) female or male flies were collected under cold anesthesia respectively. Transfer the flies into new vials containing food, and place them for 2 hr on the work surface where the experiment will be performed. The flies each group were transferred to a two-dimensional chamber at the same time of the day between 12 p.m. and 3 p.m, and then forced the flies to form a tight group, subsequently allowing

them to take their preferred distance from each other. According to the established method, for the group which any strains having climbing defects, we used horizontal chambers to test social space; however, for the group which any strains have no climbing defects, we used vertically oriented or horizontal chambers to do social space analysis. When the flies have settled, usually after around 30 min, take a picture for the social space chamber. Repeat the experiment for each genotype or condition 2–3 internal replicates and 3 independent repeats. After that, we upload the pictures to a computer and measured the nearest neighbor distances with ImageJ as the established anlaysis method (Mcneil et al., 2015). Statistical significance was evaluated using Kolmogorov-Smirnov Test of GraphPad Prism 6.0.

Direct social contacting analysis—Coordinated movements in *D. melanogaster*, such as walking and body contacting are required for many types of complex behaviors, including courtship (Greenspan and Ferveur, 2000) and social interactions (Strauss and Heisenberg, 1990). Social interactions were identified by finding sequential frames in which flies were in close proximity to each other. Based on identification of individual time periods in which flies were in close proximity, we observed social interaction behaviors using real-time tracking software (Iyengar et al., 2012). The 3 to 5-day-old specified genotype females and males were loaded individually into round two-layer chambers (diameter: 1.5 cm; height: 2.5 mm per layer). One female or one male with same genotype was put into one layer of a chamber, and then one female or male was gently aspirated into the other layer of the two-layer chamber which is separated from the target fly by a plastic transparent barrier until direct contact test was performed (20 min) (Iyengar et al., 2012). The direct social contact index indicated the percentage of observed time in which two flies interacted with one another. The direct social contact of two flies was recorded for 20 min, digitized and analyzed using Ethovision®XT software by other people different from people. To exclude any factitious factors, blinding was done during analysis process: the analyst who was not be aware of the group in which they are placed performed the social contacting analysis. Any pairs with having injured fly during the experiment process were excluded from the assay.

Social avoidance analysis of *Drosophila* stress odorant—To study social avoidance, we used assays previously described (Fernandez *et al.*, 2014). Using this assay, Fernandez et al. recently demonstrated that different genetic risks for autism have contrasting effects in social behavior (Fernandez et al., 2014). Following the established method, 2 hr before performing the experiment, we transfer the responders and emitters flies into fresh food vials to ensure that these flies are not starved and let the flies adjust to the environment for 2 hr, on the bench which the experiment. Then, we used a T-maze device to detect the avoidance of different group flies from an irritating odor. To obtain vials with dSO, we mechanically agitated a vial with 100 emitter flies on a mini-vortex as follows: vortex for 15s, remove the vial from the vortex for 5s. This process was repeated three times for a total of 60s. We removed the emitter flies out of the fresh vial and quickly placed the dSO filled vial onto one of the two sides of the T-maze apparatus. 15–40 females or males from each group (3–7 days old) were put into the T-maze, and a fresh test vial was placed on the other side of the T-maze. After the elevator was completely down, the test flies were allowed to choose between the dSO containing tube and the fresh tube for 1 min (Wise et al., 2015). The Performance Index (PI) was calculated for each genotype by subtracting the

number of flies in the dSO vial from the number of flies in the dSO-free vial, and then dividing by the total number of flies indicated as the “performance index” (Fernandez et al., 2014). Statistical significance was evaluated using t-test of GraphPad Prism 6.0. Blinding was not done during these experiments.

Lifespan Assays—Flies of the specified genotype or treatment with antibiotic food or *L. plantarum* were raised at low density (20–25 flies per vial) and three vials each group at the 25°C or 29°C (RNAi activated and control flies). Live flies were counted every day and transferred to new vials every 2 days. Survival data are presented as mean ± SEM from three vials. Lifespan experiments were carried out at least two times from independent parents. Representative lifespan experiments are shown in the Figures.

Serotonin detection—Approximately 10–20 whole bodies, abdomens, digestive tracts or heads from 3–7 days old female adult were pooled and placed in 0.2 mL PBS, and homogenized on ice for 5–10 min. Each sample was centrifuged at 3000 rpm for 20 min. The supernatants were used to perform ELISA to measure the concentration of 5-HT using the serotonin assay kit (cat. #H104, Jiancheng, Nanjing, China). The final amount of 5-HT was normalized by the total weight of flies or the number of heads or digestive tracts used for each sample. For each group, at the least three independent biological replicates were made. Statistical significance was evaluated using t-test of GraphPad Prism 6.0.

Transmission electron microscopy—Twenty sections from the digestive tracts of 3–7 days old female flies were fixed overnight at 4°C in 0.1 M phosphate buffer containing 2.5% glutaraldehyde. The samples were washed with 0.1 M phosphate buffer four times (15 min each), and postfixed with 1% osmium oxide in 0.1 M phosphate buffer for 2 hr at 4°C, followed by two washes with water (10min). The samples were stained with 2% uranyl acetate for 2 hr after which the samples were dehydrated using a graded ethanol series (50, 70, 90, and 100%) for 15 min at each concentration, followed by two rinses with 100% acetone for 15 min and embedded in araldite resin (EPON 812) and incubated overnight at 30°C. Afterwards, the samples were polymerized at 37°C for 12 hr, 45°C for 12 hr, 60°C for 48 hr. Sections (60–80 nm) were obtained with an ultramicrotome and stained with lead citrate. The sections were viewed by transmission electron microscope (FEI, Tecnai Spirit Bio TWIN, USA).

Gram-staining of gut microbiota—4 female gut digestive tracts each genotype or group in 200 μL PBS were cut into small pieces and vortex for 30s. Then, the sample was spin down for 30s at 1000 rpm.

50 μL supernatants was transferred to a slide and spread as a thin film over a circle of 1.5 cm in diameter. The suspension was air-dried and gently fixed using a flame, after which crystal violet stain was added for 60 s. Excess stain was poured and the slide was rinsed in running water. The slide was incubated in iodine solution for 60s. Excess iodine solution was removed and the slide was rinsed in running water. A few drops of decolored solution were added to the slide so the solution trickles down the slide and rinsed off with water after 20–40s. The slide was counterstained with basic fuchsin solution for 60s, washed with sterile water, air-dried, and examined under a microscope. Photographs were collected from the

four corners and the middle of the staining area, and purple-stained gram-positive bacteria and pink-stained gram-negative bacteria were identified and counted. For each group, at the least two independent biological replicates were made. Statistical significance was evaluated using t-test of GraphPad Prism 6.0.

Western blot—The total protein was extracted from 30 digestive tracts or 30 heads of 3–7 days old female adult flies using 60 μl RIPA buffer (50 mM Tris, pH 7.4, 150 mM NaCl, 1% TritonX-100, 1% sodium deoxycholate, 0.1% SDS, 2 mM sodium pyrophosphate, 25 mM β-glycerophosphate, 1 mM EDTA, 1× Protease Inhibitor Cocktail from Roch company). The same amount of protein samples were run on the SurePAGE 4–12% or 4–20% MOPS gel (GenScript) and then transferred to polyvinylidene difluoride (PVDF) membrane. After blocking non-specific sites with 5% milk or Odyssey Blocking buffer, the membrane was incubated with the different primary antibodies including KDM5 antibody((Secombe et al., 2007), Anti-H3K4me3 (Active Motif) and Anti-H3 (Abcam) at 4 C o/n, followed by incubation with HRP-conjugated secondary antibodies (Santa cruz blotechnology) or IRDye 800CW/680RD goat anti-rabbit/goat anti-mouse secondary antibodies ((LI-COR Biosciences)). Immunoreactive bands were detected using Tanon™ High-sig ECL Western Blotting Substrate(Tanon) and visualized using ChemiDoc™ Touch Imaging System or ODYSSEY INFRARED IMAGER (LI-COR) respectively. Band intensity quantities using ImageJ.

Real-time PCR—Total RNA (1 μg) which was isolated from S2 cells or 20 digestive tracts from 3–7 days old female adult flies, was reverse transcribed using the Verso cDNA kit (Thermo Scientific) with oligo (dt) primer. qRT-PCR reactions were performed in triplicate as described previously (Liu and Secombe, 2015). Primer sequences are provided in Table S1.

Plasmid construction—PGRP-LC-RE-GFP over-expressing plasmid was constructed by cloning a PGRP-LC-RE cDNA product into pAc5.1/V5-HisB-GFP using Sac II and XbaI sites. The PGRP-LC-RE cDNA fragment was PCR amplified with PGRP-LC-RE forward primer, 5'-GATCTAGAATGTCGAGGAACACGCTTGA-3' and PGRP-LC-RE reverse primer, 5'-GACCGCGGTTAGATTTCGTGTGACCAGT-3'. *imd*-GFP plasmid was constructed by cloning *imd* cDNA product into pAc5.1/V5-HisB-GFP using ApaI and XbaI sites. The *imd* cDNA fragment was amplified with *imd* forward primer, 5'-GC TCTAGAATGTCAAAGCTCAGGAACCT-3' and *imd* reverse primer, 5'-GA GGGCCCCTAGCTGTTTGTCTTGCGCTTC-3'.

Transfection—S2 cells were cultured in Schneider's *Drosophila* Medium(Gibco) and seeded in 6-well culture plates at 10^5 cells per well. S2 cells were transfected with 0.4 μg pAc5.1/V5-HisB-GFP, pAc5.1/V5-HisB-PGRP-LC-RE-GFP, pAc5.1/V5-HisB-imd-GFP using Effectene Transfection Reagent (Qiagen, USA). 24 hours after transfection, the transfected cells were collected for total RNA isolation.

Inducing *kdm5* RNAi in S2 Cells by transfection with dsRNA—The sequence of the fragment targeting 330 bp of the *kdm5* genes was amplified by PCR with the forward primer 5′-ATCAGATCGCAAAGTTCTGG-3′ and reverse primer 5′-

AATCGGTTCCACCTCCGTCCT-3′. In addition, an unrelated dsRNA *corresponding to a* green fluorescence protein *(*GFP*)* gene was used as a control, and a PCR product targeting the 413 bp region was amplified by the forward primer 5′-TGCTTTGCGAGATACCCAGA-3′ and reverse primer 5′-AGGGCAGATTGTGTGGACAG-3′. The dsRNAs synthesis templates were constructed using the PCR products with primers containing the T7 RNA polymerase promoter sequence 5′-TAATACGACTCACTATAGGG-3′. The dsRNAs were synthesized according to T7 RiboMAX™ Express RNAi System kit (Promega Corporation, Madison, WI, USA). 10 ug of kdm5-dsRNA or GFP-dsRNA was added in each well with following the previous methods (Zhou et al., 2013). After treatment for three days, S2 cells were collected and total RNA was extracted using Trizol reagent (Invitrogen, Carlsbad, CA, USA) following the manufacturer's instructions.

S2 cells with 20E and PGN treatment—S2 cells were treated with 1 μM 20-hydroxyecdysone (20E) for 24 hr or 2 μg/ml peptidoglycan (PGN) for 6 hr to activate IMD pathway as previous descriobed (Rus, F et al., 2013).

Agarose gel electrophoresis for checking open reading frame expression of *PGRP-LC* isforms—Total RNA was isolated from 20 digestive tracts of *wt* flies, *kdm5*$^{K6801/10424}$ flies, Control flies, KDM5 intestine-specific RNAi flies, KDM5^{RNAi} S2 cells and GFP^{RNAi} S2 cells respectively. All flies are female at the age of 3–5 day old. 1μg total RNA each group was reverse transcribed using the Verso cDNA kit (Thermo Scientific) with oligo (dt) primer. PCR reactions were carried out in 25 μL reactions with 12.5 μL of 2×Hieff® Robust PCR Master Mix (YESEA, China), 0.2 μM of forward and reverse primers, and 150 ng template cDNA. Thermal cycling consisted of initial denaturation at 95°C for 5 min, followed by 36 cycles of denaturation at 95°C for 30s, annealing at 55°C for 30s, and elongation at 72°C for 60s. Finally, 72°C for 5 min. PCR products were detected on 2% agarose gels by electrophoresis.

QUANTIFICATION AND STATISTICAL ANALYSIS

Unless otherwise indicated, data are presented as mean ± SEM from at least three independent biological replicates. Statistical significance was evaluated using Student's t test analyses or Kolmogorov-Smirnov test analysis by GraphPad Prism 6.0 software. Data are presented as mean ± SEM and $p < 0.05$, $p < 0.01$, $p < 0.001$ and $p<0.0001$ was considered statistically significant. The exact value of n representing the number of group in the experiments described was indicated in the figure legends. Any additional technical replicates are described within the Method Details and the results.

Supplementary Material

Refer to Web version on PubMed Central for supplementary material.

ACKNOWLEDGMENTS:

This work was supported by NSFC grant 81671983 and 81871628, Natural science funding BK20161572 from Jiangsu province and starting package from NJMU (X.L.), Young scientist funding BK20161025 from Jiangsu province (Q.L. and J.W.), Lawrence Berkeley National Laboratory Directed Research and Development (LDRD)

program funding under the Microbes to Biomes (M2B) initiative under contract DE AC02–05CH11231 (J.H.M., A.M.S. and S.E.C.), NIH grant R01GM112783 to (J.S.), and NSFC grant 31671311 (J.H.C.). The authors thank X.L. lab members, reviewers' suggestions and Tsinghua Fly Center.

REFERENCES

Anders S, Reyes A, and Huber W (2012). Detecting differential usage of exons from RNA-seq data. Genome Res 22, 2008–2017. [PubMed: 22722343]

Asong J, Wolfert MA, Maiti KK, Miller D, and Boons GJ (2009). Binding and cellular activation studies reveal that Toll-like receptor 2 can differentially recognize peptidoglycan from gram-positive and gram-negative bacteria. J. Biol. Chem 284, 8643–8653. [PubMed: 19164296]

Becker T, Loch G, Beyer M, Zinke I, Aschenbrenner AC, Carrera P, Inhester T, Schultze JL, and Hoch M (2010). FOXO-dependent regulation of innate immune homeostasis. Nature 463, 369–373. [PubMed: 20090753]

Bing X, Gerlach J, Loeb G, and Buchon N (2018). Nutrient-dependent impact of microbes on *Drosophila suzukii* development. mBio 9, e02199-17. [PubMed: 29559576]

Borghi E, Borgo F, Severgnini M, Savini MN, Casiraghi MC, and Vignoli A (2017). Rett syndrome: a focus on gut microbiota. Int. J. Mol. Sci 18, 344.

Bosco-Drayon V, Poidevin M, Boneca IG, Narbonne-Reveau K, Royet J, and Charroux B(2012). Peptidoglycan sensing by the receptor PGRP-LE in the *Drosophila* gut induces immune responses to infectious bacteria and tolerance to microbiota. Cell Host Microbe 12, 153–165. [PubMed: 22901536]

Broderick NA, Buchon N, and Lemaitre B (2014). Microbiota-induced changes in *Drosophila melanogaster* host gene expression and gut morphology. mBio 5, e01117–14.

Broderick NA, and Lemaitre B (2012). Gut-associated microbes of *Drosophila melanogaster*. Gut Microbes 3, 307–321. [PubMed: 22572876]

Brookes E, Laurent B, Ounap K, Carroll R, Moeschler JB, Field M, Schwartz CE, Gecz J, and Shi Y (2015). Mutations in the intellectual disability gene KDM5C reduce protein stability and demethylase activity. Hum. Mol. Genet 24, 2861–2872. [PubMed: 25666439]

Bross TG, Rogina B, and Helfand SL (2005). Behavioral, physical, and demographic changes in *Drosophila* populations through dietary restriction. Aging Cell 4, 309–317. [PubMed: 16300483]

Buchon N, Broderick NA, and Lemaitre B (2013). Gut homeostasis in a microbial world: insights from *Drosophila melanogaster*. Nat. Rev. Microbiol 11, 615–626. [PubMed: 23893105]

Caporaso JG, Kuczynski J, Stombaugh J, Bittinger K, Bushman FD, Costello EK, Fierer N, Peña AG, Goodrich JK, and Gordon JI (2010). QIIME allows analysis of high-throughput community sequencing data. Nat. Methods 7, 335. [PubMed: 20383131]

Caracciolo B, Xu W, Collins S, and Fratiglioni L (2014). Cognitive decline, dietary factors and gut-brain interactions. Mech. Ageing Dev 136, 59–69. [PubMed: 24333791]

Chen K, Chen Z, Wu D, Zhang L, Lin X, Su J, Rodriguez B, Xi Y, Xia Z, and Chen X (2015). Broad H3K4me3 is associated with increased transcription elongation and enhancer activity at tumor-suppressor genes. Nat. Genet 47, 1149–1157. [PubMed: 26301496]

Chen R, Davis LK, Guter S, Wei Q, Jacob S, Potter MH, Cox NJ, Cook EH, Sutcliffe JS, and Li B (2017). Leveraging blood serotonin as an endophenotype to identify de novo and rare variants involved in autism. Mol. Autism 8, 14. [PubMed: 28344757]

Choe KM, Werner T, Stoven S, Hultmark D, and Anderson KV (2002). Requirement for a peptidoglycan recognition protein (PGRP) in Relish activation and antibacterial immune responses in *Drosophila*. Science 296, 359–362. [PubMed: 11872802]

Clark RI, Salazar A, Yamada R, Fitzgibbon S, Morselli M, Alcaraz J, Rana A, Rera M, Pellegrini M, and Ja WW (2015). Distinct shifts in microbiota composition during *Drosophila* aging impair intestinal function and drive mortality. Cell Rep 12, 1–12. [PubMed: 26119736]

Clarke G, Stilling RM, Kennedy PJ., Stanton C, Cryan JF, and Dinan TG (2014). Minireview: gut microbiota: the neglected endocrine organ. Mol. Endocrinol 28, 1221–1238. [PubMed: 24892638]

Drelon C, Belalcazar HM, and Secombe J (2018). The histone demethylase KDM5 is essential for larval growth in *Drosophila*. Genetics 209, 773–787. [PubMed: 29764901]

Dylan SJ, and Bordenstein SR (2016). Speciation by Symbiosis: the microbiome and behavior. mBio 7, e01785.

Fernandez RW, Nurilov M, Feliciano O, McDonald IS, and Simon AF (2014). Straightforward assay for quantification of social avoidance in *Drosophila melanogaster*. J. Vis. Exp 94, e52011.

Fieremans N, Esch HV, Ravel TD, Driessche JV, Belet S, Bauters M, and Froyen G (2015). Microdeletion of the escape genes KDM5C and IQSEC2 in a girl with severe intellectual disability and autistic features. Eur. J. Med. Genet 58, 324–327.

Fukuyama H, Verdier Y, Guan Y, Makino-Okamura C, Shilova V, Liu X, Maksoud E, Matsubayashi J, Haddad I, Spirohn K, et al. (2013). Landscape of protein-protein interactions in *Drosophila* immune deficiency signaling during bacterial challenge. Proc. Natl. Acad. Sci. U S A 110, 10717–10722. [PubMed: 23749869]

Greenspan RJ, and Ferveur JF (2000). Courtship in *Drosophila*. Annu. Rev. Genet 34, 205–232. [PubMed: 11092827]

Han G, Lee HJ, Jeong SE, Jeon CO, and Hyun S (2017). Comparative analysis of *Drosophila melanogaster* gut microbiota with respect to host strain, sex, and age. Microb. Ecol 74, 1–10. [PubMed: 28074246]

Hetru C, and Hoffmann JA(2009). NF-kappaB in the immune response of *Drosophila*. Cold Spring Harb. Perspect Biol 1, a000232. [PubMed: 20457557]

Houtz PL, and Buchon N (2014). Methods to assess intestinal stem cell activity in response to microbes in *Drosophila melanogaster*. Methods Mol. Biol 1213,171-182. [PubMed: 25173382]

Huang DW, Sherman BT, and Lempicki RA (2009). Systematic and integrative analysis of large gene lists using DAVID bioinformatics resources. Nat. Protoc 4, 44–57. [PubMed: 19131956]

Iyengar A, Imoehl J, Ueda A, Nirschl J, and Wu CF (2012). Automated quantification of locomotion, social interaction, and mate preference in *Drosophila* mutants. J. Neurogenet 26, 306–316. [PubMed: 23106154]

Iwase S, Brookes E, Agarwal S, Badeaux AI, Ito H, Vallianatos CN, Tomassy GS, Kasza T, Lin G, Thompson A, et al. (2016). A mouse model of X-linked intellectual disability associated with impaired removal of histone methylation. Cell Rep 14, 1000–1009. [PubMed: 26804915]

Jones RM, and Neish AS (2017). Redox signaling mediated by the gut microbiota. Free Radic. Biol. Med 105, 41–47. [PubMed: 27989756]

Kenmoku H, Ishikawa H, Ote M, Kuraishi T, and Kurata S (2016). A subset of neurons controls the permeability of the peritrophic matrix and midgut structure in *Drosophila* adults. J. Exp. Biol 219, 2331–2339. [PubMed: 27229474]

Kim D, Pertea G, Trapnell C, Pimentel H, Kelley R, Salzberg SL (2013). TopHat2: accurate alignment of transcriptomes in the presence of insertions, deletions and gene fusions. Genome Biol 14, R36. [PubMed: 23618408]

Koemans TS, Kleefstra T,Chubak MC, Stone MH, Reijnders MRF, de Munnik S, Willemsen MH, Fenckova M, Stumpel C, Bok LA, et al. (2017). Functional convergence of histone methyltransferases EHMT1 and KMT2C involved in intellectual disability and autism spectrum disorder. PLoS Genet 13, e1006864. [PubMed: 29069077]

Lee KA, and Lee WJ (2014). *Drosophila* as a model for intestinal dysbiosis and chronic inflammatory diseases. Dev. Comp. Immunol 42, 102–110. [PubMed: 23685204]

Liu XY, and Secombe J (2015). The histone demethylase KDM5 activates gene expression by recognizing chromatin context through its PHD reader motif. Cell Rep 13, 2219–2231. [PubMed: 26673323]

Liu XY, Greer C, and Secombe J (2014). KDM5 interacts with Foxo to modulate cellular levels of oxidative stress. PLoS Genet 10, e1004676. [PubMed: 25329053]

Martin HC, Jones WD, McIntyre R, Sanchez-Andrade G,Sanderson M, Stephenson JD, Jones CP, Handsaker J, Gallone G, Bruntraeger M, et al. (2018). Quantifying the contribution of recessive coding variation to developmental disorders.Science 362, 1161–1164. [PubMed: 30409806]

Mayer EA, Padua D, and Tillisch K (2014). Altered brain-gut axis in autism: comorbidity or causative mechanisms? Bioessays 36, 933–939. [PubMed: 25145752]

Mcneil AR, Jolley SN, Akinleye AA, Nurilov M, Rouzyi Z, Milunovich AJ, Chambers MC, and Simon AF (2015). Conditions affecting social space in *Drosophila melanogaster*. J. Vis. Exp 105, e53242.

Navarro-Costa P, McCarthy A, Prudencio P, Greer C, Guilgur LG, Becker JD, Secombe J, Rangan P, and Martinho RG (2016). Early programming of the oocyte epigenome temporally controls late prophase I transcription and chromatin remodelling. Nat. Commun 7, 12331. [PubMed: 27507044]

Nithianantharajah J, Balasuriya GK, Franks AE, and Hill-Yardin EL (2017). Using animal models to study the role of the gut-brain axis in autism. Curr. Dev. Disord. Rep 4, 28–36. [PubMed: 28680792]

Neyen C, Runchel C, Schüpfer F, Meier P and Lemaitre B (2016). The regulatory isoform rPGRP-LC induces immune resolution via endosomal degradation of receptors. Nat. Immunol 10, 1150.

Ptaschinski C, Mukherjee S, Moore ML, Albert M, Helin K, Kunkel SL, and Lukacs NW (2015). RSV-induced H3K4 demethylase KDM5B leads to regulation of dendritic cell-derived innate cytokines and exacerbates pathogenesis in vivo. PLoS Pathog 11, e1004978. [PubMed: 26083387]

Qian Y, Cao Y, Deng B, Yang G, Li J, Xu R, Zhang D, Huang J, and Rao Y (2017). Sleep homeostasis regulated by 5HT2b receptor in a small subset of neurons in the dorsal fan-shaped body of *Drosophila*. eLife 6, e26519. [PubMed: 28984573]

Ramdya P, Schneider J, and Levine JD(2017). The neurogenetics of group behavior in *Drosophila melanogaster*. J. Exp. Biol 220, 35–41. [PubMed: 28057826]

Rus F, Flatt T, Tong M, Aggarwal K, Okuda K, Kleino A, Yates E, Tatar M, and Silverman N (2013). Ecdysone triggered PGRP-LC expression controls *Drosophila* innate immunity. EMBO J 32, 1626–1638. [PubMed: 23652443]

Ryu JH, Kim SH, Lee HY, Bai JY, Nam YD, Bae JW, Lee DG, Shin SC, Ha EM, and Lee WJ (2008). Innate immune homeostasis by the homeobox gene caudal and commensal-gut mutualism in *Drosophila*. Science 319, 777–782. [PubMed: 18218863]

Sebald J, Willi M, Schoberleitner I, Krogsdam A, Orth-Holler D, Trajanoski Z, and Lusser A (2016). Impact of the chromatin remodeling factor CHD1 on gut microbiome composition of *Drosophila melanogaster*. PLoS One 11, e0153476. [PubMed: 27093431]

Scandaglia M, Lopez-Atalaya JP, Medrano-Fernandez A, Lopez-Cascales MT, Del Blanco B, Lipinski M, Benito E, Olivares R, Iwase S, Shi Y, et al. (2017). Loss of KDM5C causes spurious transcription and prevents the fine-tuning of activity-regulated enhancers in neurons. Cell Rep 21, 47–59. [PubMed: 28978483]

Secombe J, Li L, Carlos L, and Eisenman RN (2007). The Trithorax group protein Lid is a trimethyl histone H3K4 demethylase required for dMyc-induced cell growth. Genes Dev 21, 537–551. [PubMed: 17311883]

Shailesh H, Gupta I, Sif S, and Ouhtit A(2016). Towards understanding the genetics of autism. Front. Biosci 8, 412–426.

Snijders AM, Langley SA, Kim YM, Brislawn CJ, Noecker C, Zink EM, Fansler SJ, Casey CP, Miller DR, Huang Y, et al. (2016). Influence of early life exposure, host genetics and diet on the mouse gut microbiome and metabolome. Nat. Microbiol 2, 16221. [PubMed: 27892936]

Strauss R, and Heisenberg M (1990). Coordination of legs during straight walking and turning in *Drosophila melanogaster*. J. Comp. Physiol. A 167, 403–412. [PubMed: 2121965]

Thaiss CA, Zmora N, Levy M, and Elinav E (2016). The microbiome and innate immunity. Nature 535, 65–74. [PubMed: 27383981]

Tynkkynen S, Singh KV, and Varmanen P (1998). Vancomycin resistance factor of *Lactobacillus rhamnosus* GG in relation to enterococcal vancomycin resistance (van) genes. Int. J. Food Microbiol 47,195–204.

Venu I, Durisko Z, Xu J, and Dukas R (2014). Social attraction mediated by fruit flies' microbiome. J. Exp. Biol 217, 1346–1352. [PubMed: 24744425]

Wang J, Thingholm LB, Skieceviciene J, Rausch P, Kummen M, Hov JR, Degenhardt F, Heinsen FA, Ruhlemann MC, Szymczak S, et al. (2016). Genome-wide association analysis identifies variation in vitamin D receptor and other host factors influencing the gut microbiota. Nature genetics 48, 1396–1406 [PubMed: 27723756]

Wei GZ, Deng XX, Agarwal S, Iwase S, Disteche C, and Xu J (2016). Patient mutations of the intellectual disability gene KDM5C downregulate netrin G2 and suppress neurite growth in Neuro2a cells. J. Mol. Neurosci 60, 33–45. [PubMed: 27421841]

Wise A, Tenezaca L, Fernandez RW, Schatoff E, Flores J, Ueda A, Zhong X, Wu CF, Simon AF, and Venkatesh T (2015). *Drosophila* mutants of the autism candidate gene neurobeachin (rugose) exhibit neuro-developmental disorders, aberrant synaptic properties, altered locomotion, impaired adult social behavior and activity patterns. J. Neurogenet 29, 135. [PubMed: 26100104]

Wong AC, Dobson AJ, and Douglas AE (2014). Gut microbiota dictates the metabolic response of *Drosophila* to diet. J. Exp. Biol 217, 1894–1901. [PubMed: 24577449]

Wu SC, Cao ZS, Chang KM, and Juang JL (2017). Intestinal microbial dysbiosis aggravates the progression of Alzheimer's disease in *Drosophila*. Nat. Commun 8, 24. [PubMed: 28634323]

Zamurrad S, Hatch HAM, Drelon C, Belalcazar HM, and Secombe J (2018). A *Drosophila* model of intellectual disability caused by mutations in the histone demethylase KDM5. Cell Rep 22, 2359–2369. [PubMed: 29490272]

Zhai Z, Huang X, and Yin Y (2018). Beyond immunity: the Imd pathway as a coordinator of host defense, organismal physiology and behavior. Dev. Comp. Immunol 83, 51–59. [PubMed: 29146454]

Zhou R, Mohr S, Hannon GJ, and Perrimon N (2013). Inducing RNAi in *Drosophila* cells by transfection with dsRNA. Cold Spring Harb. Protoc 5, 461–463.

Highlights:

- Deficiency of KDM5 demethylase causes gut dysbiosis and abnormal social behavior in flies.
- *Lactobacillus plantarum* administration improves social behavior in *kdm5*-deficient animals.
- KDM5 maintains proper immune activity in a transcriptional and microbiota-mediated manner.
- KDM5 demethylase affects social behavior through the gut-microbiome-brain axis.

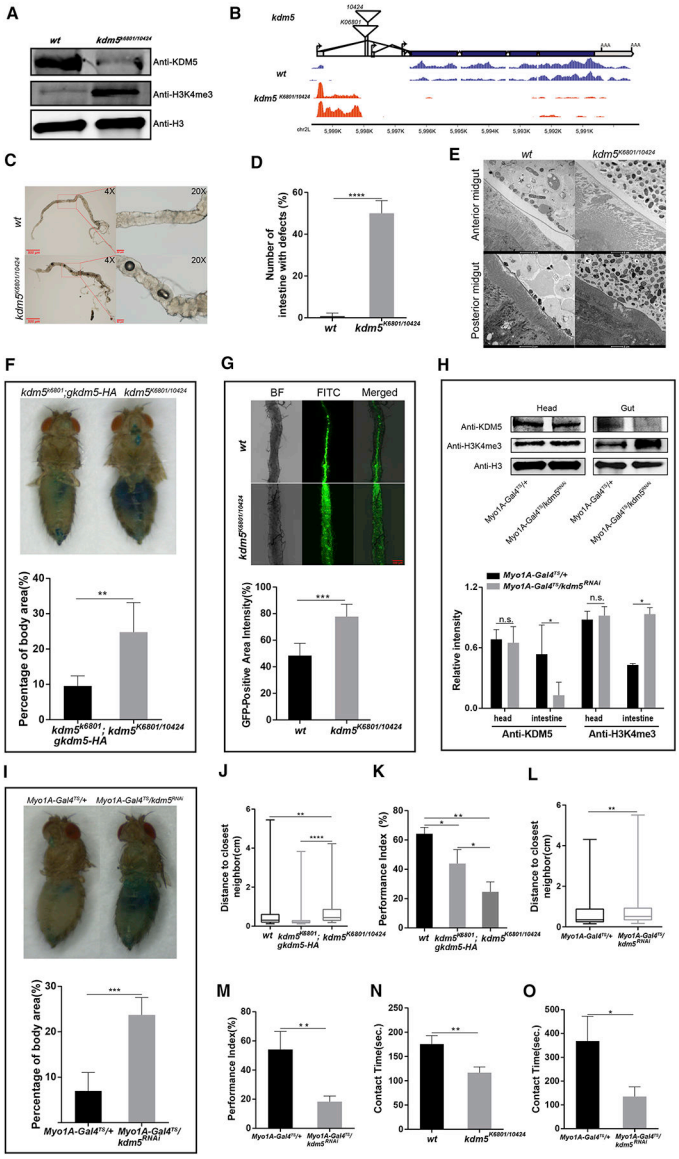

Figure 1. Loss of KDM5 causes intestinal epithelial barrier disruption and impaired social behavior.

A. Levels of KDM5, H3K4me3 and Histone H3 in intestine tissues from wildtype (*wt*, w^{1118}) and $kdm5^{K6801/10424}$ flies using Western blot analysis.

B. Transcription levels of *kdm5* in intestine tissues from *wt* and $kdm5^{K6801/10424}$ flies using RNA-seq analysis.

C. Representative images of the digestive tract from *wt* and $kdm5^{K6801/10424}$ flies (left panel, 4×). The red dotted box highlights a portion of the midgut showing intestinal defects with bubbles in $kdm5^{K6801/10424}$ flies compared to *wt* (right panel 20×).

D. Percentage of flies with intestinal defects with bubbles in *wt* and $kdm5^{K6801/10424}$ flies at the age of 3–5 days. In total, 30–40 flies each group were examined.

E. Transmission electron micrographs of the epithelial barrier in the anterior (top-panel) and posterior (bottom-panel) midgut from *wt* and $kdm5^{K6801/10424}$ flies (2.9K magnification).

F. Intestinal permeability analysis for *wt* and $kdm5^{K6801/10424}$ flies was assessed by measuring the post-feeding distribution of a non-absorbable blue food dye (top-panel). Quantification of the percentage of body area with distribution of non-absorbable blue food dye relative to whole body (bottom panel).

G. The digestive tract of $kdm5^{K6801/10424}$ flies are highly permeable. Conventional fluorescence microscopy revealed that FITC-labeled beads remained in the lumen of wild-type flies after feeding. In contrast, FITC signals were diffuse in the gut of $kdm5^{K6801/10424}$ flies.

H. Protein Levels of KDM5, H3K4me3 and Histone H3 in heads and intestine tissues from $Myo1A\text{-}Gal4^{TS}/+$ and $Myo1A\text{-}Gal4^{TS}/kdm5^{RNAi}$ flies using Western blot analysis (top panel). Quantification of intensity for western blot is shown in the bottom panel.

I. Post-feeding distribution of a non-absorbable blue food dye in $Myo1A\text{-}Gal4^{TS}/+$ and $Myo1A\text{-}Gal4^{TS}/kdm5^{RNAi}$ flies to measure intestinal permeability. Quantification of the percentage of body area with distribution of non-absorbable blue food dye relative to whole body.

J. $kdm5^{K6801ñ0424}$ flies showed an increase in social space compared to *wt* and *kdm5* rescued flies.

K. Social avoidance analysis showed a decrease activity for $kdm5^{K6801/10424}$ flies compared to *wt* and *kdm5* rescued flies.

L. Distribution of social space in control $Myo1A\text{-}Gal4^{TS}$ and $Myo1A\text{-}Gal4^{TS}/kdm5^{RNAi}$ flies. $Myo1A\text{-}Gal4^{TS}/kdm5^{RNAi}$ flies showed an increase in social space compared to control.

M. Social avoidance analysis showed decreased activity in $Myo1A\text{-}Gal4^{TS}/kdm5^{RNAi}$ flies compared to *control*.

N. Direct social contacting time was reduced in female $kdm5^{K6801/10424}$ flies compared to *wt*.

O. Direct social contacting time was reduced in male $Myo1A\text{-}Gal4^{TS}/kdm5^{RNAi}$ compared to *control*.

Error bars represent minimum and maximum (J and L). Other data are shown as mean ± SEM. n = 3 (J–M). n>8 (N and O). $*p < 0.05$, $**p < 0.01$, and $***p < 0.001$. In total, 10–15 flies in each group were examined (F, G, and I). Data shown in (D) and (F)–(I) are representative of two independent experiments.

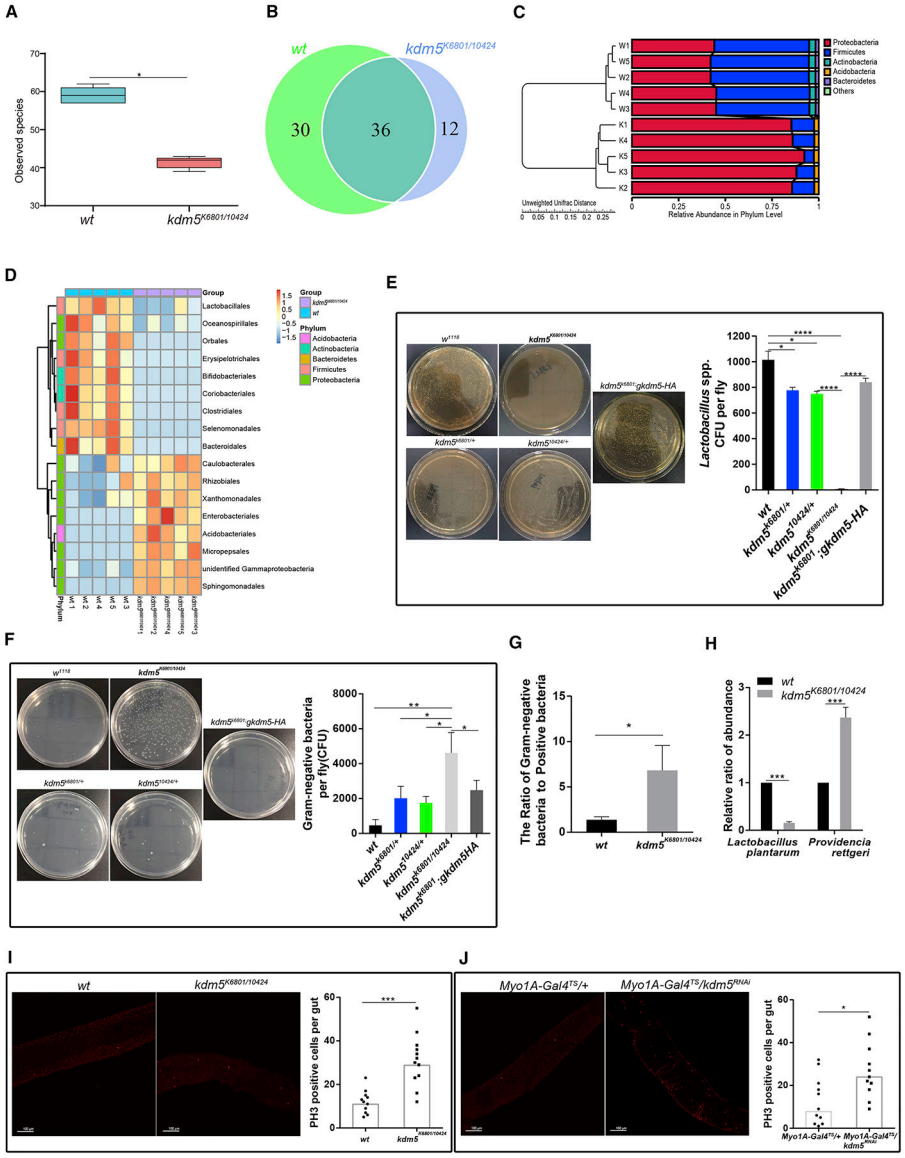

Figure 2. Loss of KDM5 protein alters gut microbiota composition.

A. Observed bacterial species richness in gut samples from *wt* and *kdm5*$^{K6801/10424}$ flies. *P* value<0.05 by Wilcoxon rank sum test.

B. Overlap of observed bacterial OUTs in gut samples from *wt* and *kdm5*$^{K6801/10424}$ flies.

C. Hierarchical clustering of *wt* and *kdm5*$^{K6801/10424}$ flies using Bray-Curtis dissimilarity indices at the phylum level by the unweighted unifrac distances.

D. Heatmap of normalized relative abundance levels of OTUs significantly changed between *wt* and *kdm5*$^{K6801/10424}$ flies grouped into 17 orders and colored at the phylum level (Wilcoxon rank sum test, P<0.05).

E. *Lactobacillus* spp. loading was determined by plating 3-day old wt, *kdm5*^{10424}, *kdm5*^{K06801}, *kdm5*$^{K6801/10424}$, and *kdm5*^{k6801}*;gkdm5-HA* fly intestine samples on De Man, Rogosa, and Sharpe (MRS) agar at 37°C.

F. Gram-negative bacteria loading was determined by plating 4-day old *wt*, $kdm5^{10424}$, $kdm5^{K06801}$, $kdm5^{K6801/10424}$, and $kdm5^{k6801}$;*gkdm5-HA* fly intestine samples on selective Gram-negative bacteria agar at 25°C.

G. The ratio of gram-negative to gram-positive bacteria in intestinal samples of $kdm5^{K6801/10424}$ and *wt* flies.

H. Q-PCR analysis showing the abundance level of *L. piantarum* L168 and *P. rettgeri* P6 in intestinal samples *of* $kdm5^{K6801/10424}$ and *wt* flies.

I. The number of PH3 positive staining stem cells in mid-gut samples from $kdm5^{K6801/10424}$ and *wt* flies.

J. The number of PH3 positive staining stem cells in mid-gut samples from *Myo1A-*$Gai4^{TS}$/ $kdm5^{RNAi}$ and *wt* flies.

Data are shown as mean ± SEM. n ≥ 3 (A-G). 10–20 flies were examined each group (I and J). Data shown in (H-J) are representative of two independent experiments.* P <0.05; ** P < 0.01 and *** P < 0.001.

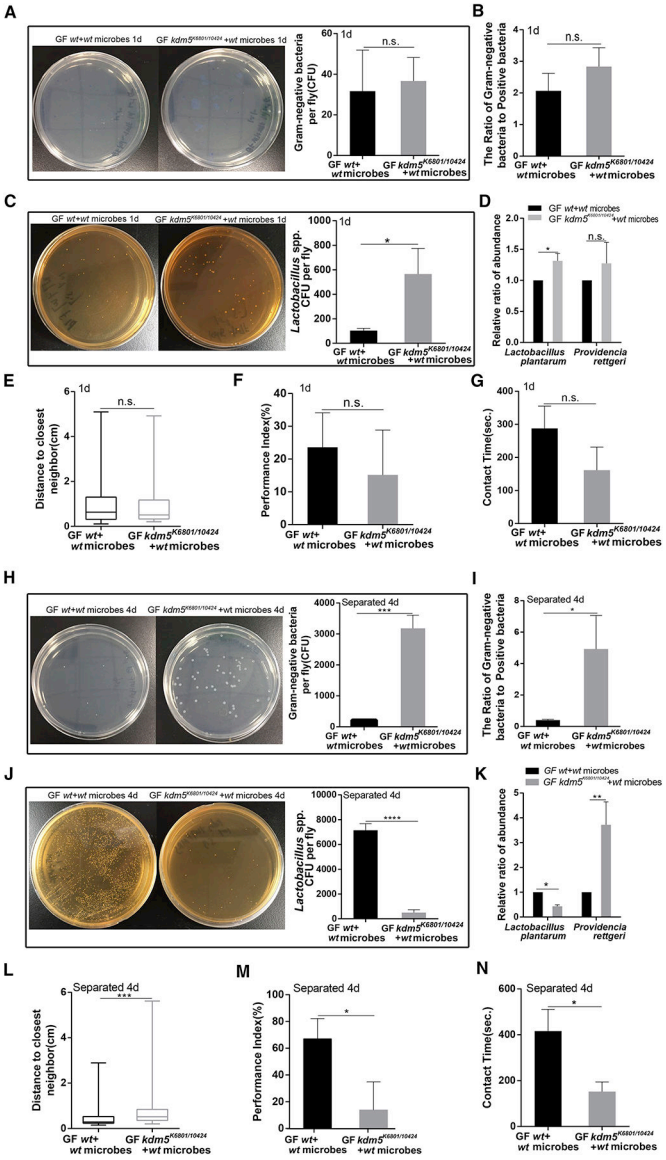

Figure 3. Gut bacterial and behavior analysis of GF *wt* and GF *kdm5*^{K680110424} flies reconstituted with microbiome isolated from *wt* flies

A. Gram negative bacteria abundance in 1 day old GF *wt and kdm5*$^{K6801/10424}$ flies reconstituted with microbes from *wt* flies at 25°0.

B. The ratio of gram-negative to gram-positive cells in 1 day old GF *wt and kdm5*$^{K6801/10424}$ flies reconstituted with microbes from *wt* flies.

C. *Lactobacillus* spp. bacteria abundance in 1 day old GF *wt and kdm5*$^{K6801/10424}$ flies reconstituted with microbes from *wt* flies.

D. Real-time PCR analysis of abundance of *L. piantarnm* L168 and *P. rettgeri P6* in 1 day old GF *wt and kdm5*$^{K6801/10424}$ flies reconstituted with microbes from *wt* flies.

E. Social space in 1 day old GF *wt and kdm5*$^{K6801/10424}$ flies reconstituted with microbes from *wt* flies.

F. Social avoidance (performance index) in 1 day old GF *wt and kdm5*$^{K6801/10424}$ flies reconstituted with microbes from *wt* flies.

G. Direct social contacting time in 1 day old GF *wt and kdm5*$^{K6801/10424}$ flies reconstituted with microbes from *wt* flies.

H. Gram negative bacteria abundance in 4 days old GF *wt and kdm5*$^{K6801/10424}$ flies reconstituted with microbes from *wt* flies.

I. The ratio of gram-negative to gram-positive cells in 4 days old GF *wt and kdm5*$^{K6801/10424}$ flies reconstituted with microbes from *wt* flies.

J. *Lactobacillus* spp. bacteria abundance in 4 days old GF *wt and kdm5*$^{K6801/10424}$ flies reconstituted with microbes from *wt* flies.

K. Real-time PCR analysis of abundance of *L. plantarum* L168 and *P. rettgeri P6* in 4 day old GF *wt and kdm5*$^{K6801/10424}$ flies reconstituted with microbes from *wt* flies.

L. Social space in 4 days old GF *wt and kdm5*$^{K6801/10424}$ flies reconstituted with microbes from *wt* flies.

M. Social avoidance (performance index) in 4 days old GF *wt and kdm5*$^{K6801/10424}$ flies reconstituted with microbes from *wt* flies.

N. Direct social contacting time in 4 days old GF *wt and kdm5*$^{K6801/10424}$ flies reconstituted with microbes from *wt* flies.

Error bars represent min and max (E and L). Other Data are shown as mean ± SEM. n ≥ 3 (A-C, E, F,H-J, L and M). n≥8 (G and N). n=2 (D,K). *$P < 0.05$, **$P < 0.01$, ***$P < 0.001$ and ****$p < 0.0001$. ns, not significant.

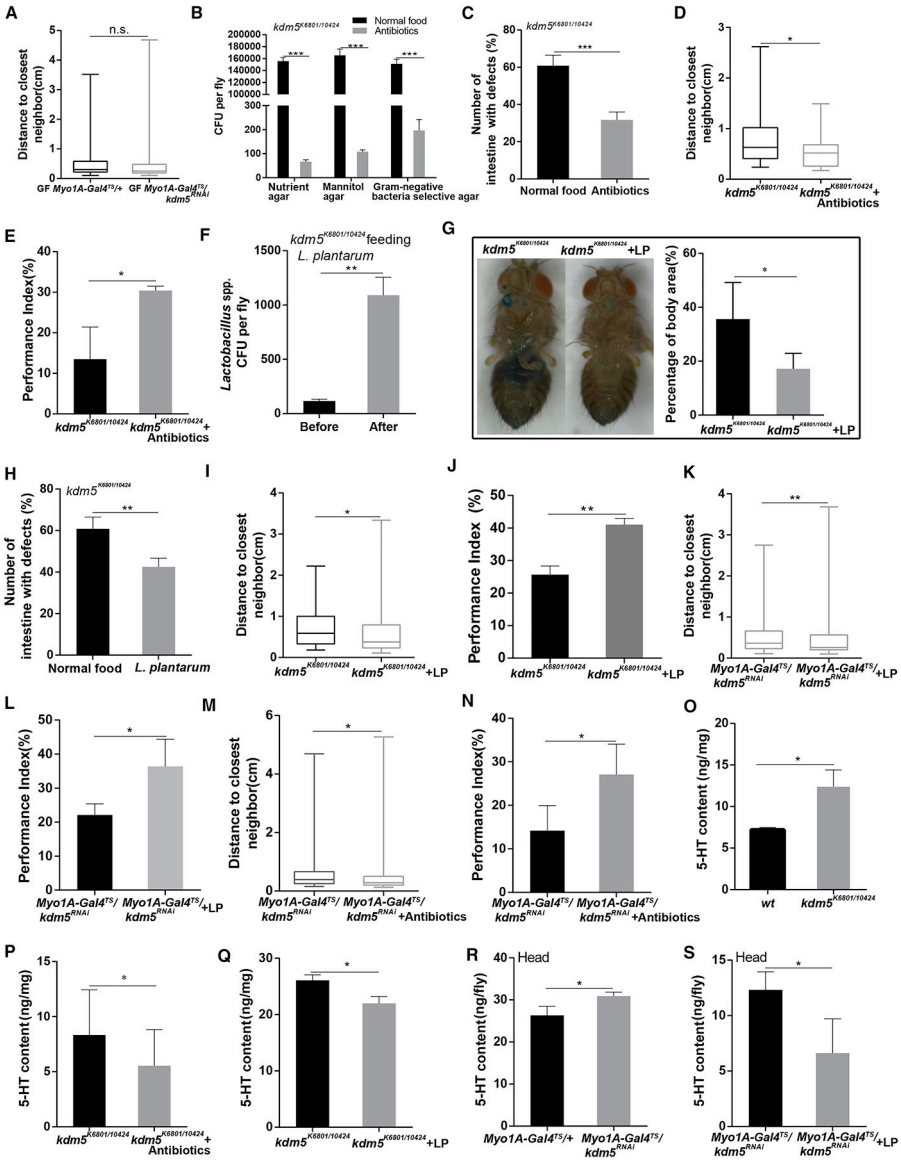

Figure 4. KDM5 manipulates the microbial composition to affect social behavior.

A. Social space in GF *Myo1A-Gal4^{TS}/kdm5^{RNAi}* and GF control *flies*.

B. Pathogenic-like bacteria isolated from *kdm5$^{K6801/10424}$* flies fed with antibiotic fortified food or standard food cultured on nutrient agar, mannitol agar and gram-negative bacteria agar at 25°C.

C. Intestinal defects with bubbles in *kdm5$^{K6801/10424}$* flies fed with antibiotic fortified food or standard food.

D. Social space in *kdm5$^{K6801/10424}$* flies fed with antibiotic fortified food or standard food.

E. Social avoidance (performance index) in *kdm5$^{K6801/10424}$* flies fed with antibiotic fortified food or standard food.

F. Abundance of *Lactobacillus* spp. isolated from gut samples of *kdm5$^{K6801/10424}$* flies maintained on food supplemented with *Lactobacillus* spp. or standard food.

G. Intestinal permeability assay in *kdm5*$^{K6801/10424}$ flies maintained on food supplemented with *L. plantarum* L168 or standard food.
H. Intestinal defects with bubbles in *kdm5*$^{K6801/10424}$ flies maintained on food supplemented with *L. plantarum* L168 or standard food.
I. Social space in *kdm5*$^{K6801/10424}$ flies maintained on food supplemented with *L. plantarum* L168 or standard food.
J. Social avoidance (performance index) in *kdm5*$^{K6801/10424}$ flies maintained on food supplemented with *L. plantarum* L168 or standard food.
K. Social space in *Myo1A-Gal4*^{TS}/*kdm5*^{RNAi} flies maintained on food supplemented with *L. plantarum* L168 or standard food.
L. Social avoidance (performance index) in *Myo1A-Gal4*^{TS}/*kdm5*^{RNAi} flies maintained on food supplemented with *L. plantarum* L168 or standard food.
M. Social space in *Myo1A-Gal4*^{TS}/*kdm5*^{RNAi} flies treated with or without antibiotics.
N. Social avoidance (performance index) in *Myo1A-Gal4*^{TS}/*kdm5*^{RNAi} flies treated with or without antibiotics.
O. Concentration of 5-HT in abdomens samples from *wt* and *kdm5*$^{K6801/10424}$ flies.
P. Concentration of 5-HT in abdomens samples from *kdm5*$^{K6801/10424}$ flies treated with or without antibiotics.
Q. Concentration of 5-HT in abdomens samples from *kdm5*$^{K6801/10424}$ flies treated with *L. plantarum* L168 or standard food.
R. Concentration of 5-HT in heads of *Myo1A-Gal4*^{TS}/*kdm5*^{RNAi} and control flies.
S. Concentration of 5-HT in heads of *Myo1A-Gal4*^{TS}/*kdm5*^{RNAi} flies treated with *L. plantarum* L168 or standard food.
Error bars represent min and max (A, D, I, K, M). Other data are shown as mean ± SEM; n ≥ 3 (A, B, D-F and I-S). 30–40 flies each group were examined (C and H). Data shown in C, G and H are representative of two independent experiments. * P <0.05, ** P < 0.01 and *** P<0.001.

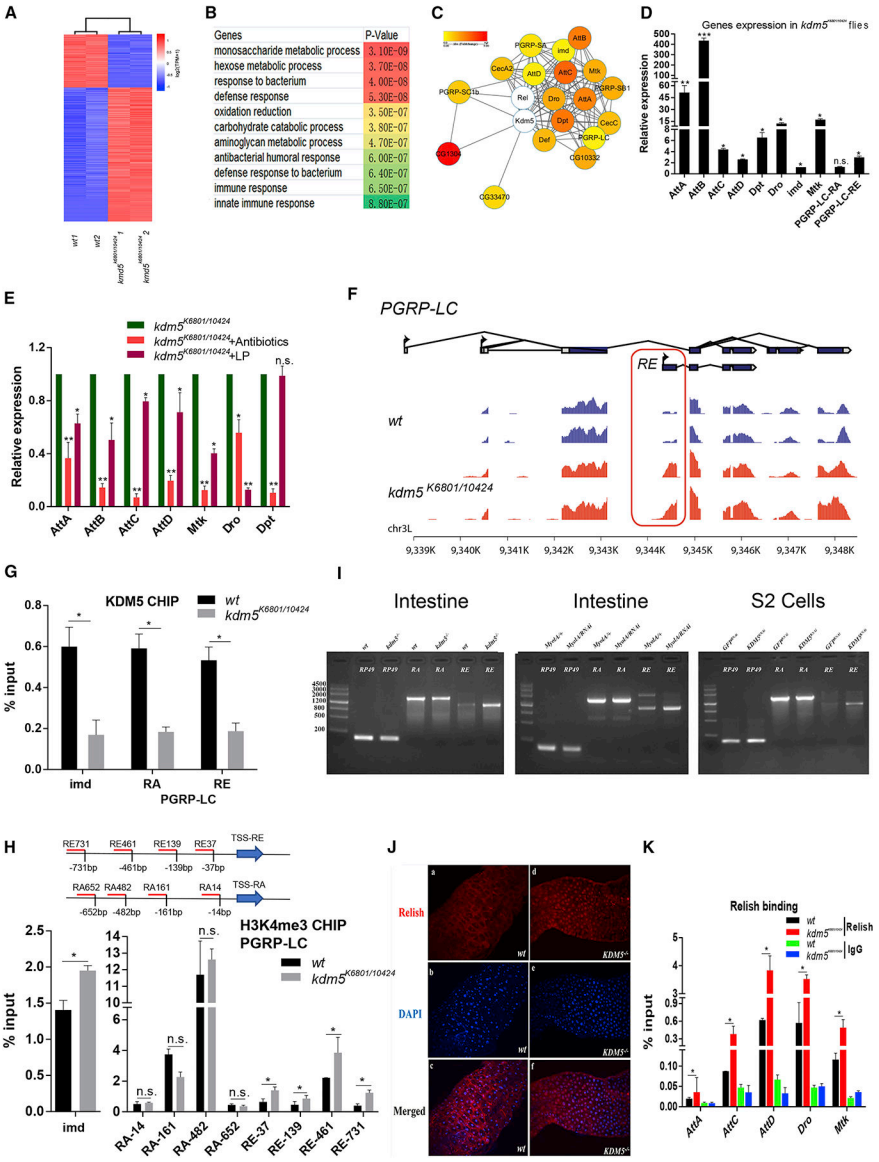

Figure 5. KDM5 negatively regulates IMD/Rel signaling.

A. Hierarchical clustering analysis of differentially expressed genes comparing *wt* and *kdm5*$^{K6801/10424}$ fly intestinal tissues. Up-regulated genes are shown in red; down-regulated genes in blue (P<0.05; fold-change ≥1.5).

B. Gene ontology biological process enrichment analysis of up- and down-regulated genes comparing *wt* and *kdm5*$^{K6801/10424}$ fly intestinal tissues.

C. Protein interaction network analysis of differentially expressed genes comparing *wt* and *kdm5*$^{K6801/10424}$ fly intestinal tissues. Node colors increasing from yellow to red indicate expression level changes in *kdm5*$^{K6801/10424}$ flies compared to *wt*.

D. Expression levels of the antimicrobial and innate immune response genes in the intestinal tissues of *kdm5*$^{K6801/10424}$ flies relative to *wt* flies were confirmed by real-time PCR.

E. Relative expression levels of antimicrobial genes in the intestinal tissues of *kdm5*$^{K6801/10424}$ female flies with *L. plantarum* L168 feeding or antibiotic treatment compared to that of *kdm5*$^{K6801/10424}$ respectively.

F. *PGRP-LC* gene structure and transcriptional profiling of intestinal samples from *wt* and *kdm5*$^{K6801/10424}$ flies.

G. ChIP-qPCR analysis of KDM5 levels at the promoter regions of *imd, PGRP-LC-RA* and *PGRP-LC-RE* genes in *wt* and *kdm5*$^{K6801/10424}$ flies intestine tissue.

H. ChIP-qPCR analysis of H3K4me3 levels at promoter regions of *imd* (left panel), *PGRP-LC-RA* and *PGRP-LC-RE* in *wt* and *kdm5*$^{K6801/10424}$ flie intestine tissue (right panel).

I. RT-PCR analysis of full-length *PGRP-LC-RA* and *PGRP-LC-RE* in S2 cells and intestinal tissue of *kdm5*$^{K6801/10424}$ and *Myo1A-Gal4*^{TS}*/kdm5*^{RNAi} flies.

J. Immunofluorescence staining of Relish in intestinal tissue of *wt* and *kdm5*$^{K6801/10424}$ flies.

K. ChIP-qPCR analysis of Relish levels at promoter regions of Relish target genes in *wt* and *kdm5*$^{K6801/10424}$ flies. IgG is included as a negative control (*$P < 0.05$). Data are shown as mean ± SEM; n ≥ 2 (A, D-I and K). *$P < 0.05$, **$P < 0.01$ and *** $P < 0.001$.

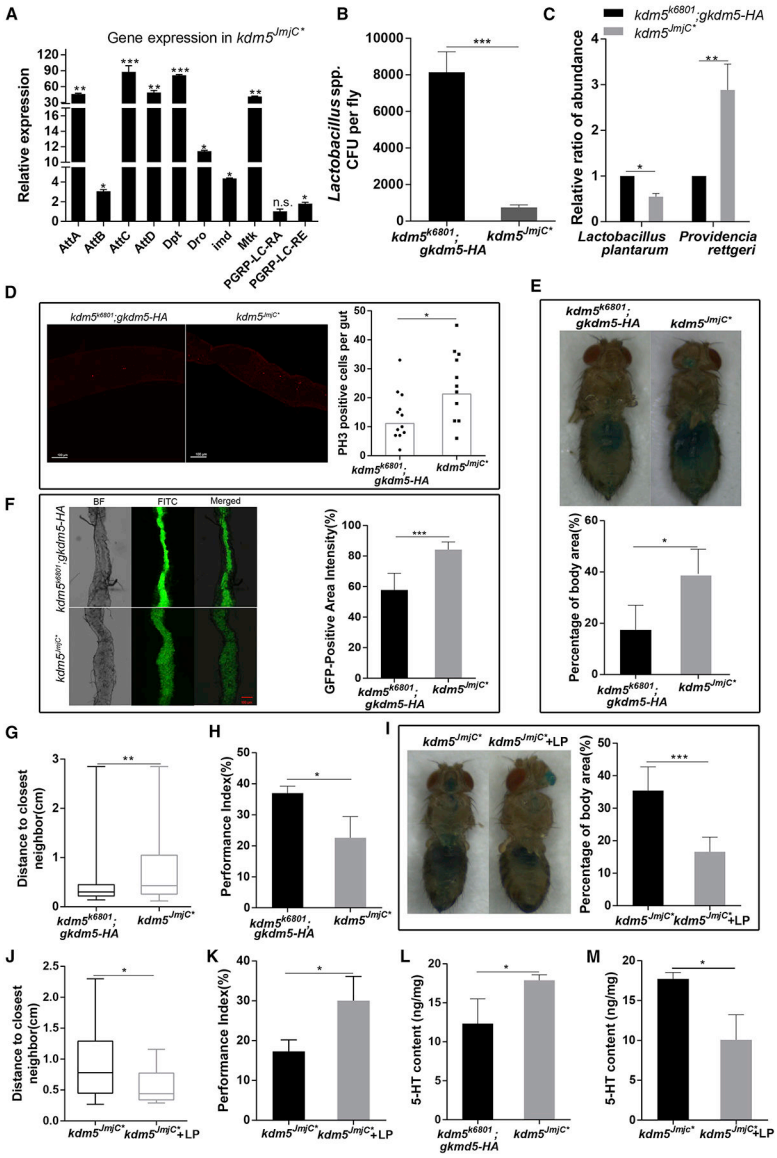

Figure 6. KDM5 demethylase activity regulates IMD/Rel pathway activity and gut microbiome-brain function

A. Expression levels of the antimicrobial and innate immune response genes of intestinal tissues from 3–5 day old *kdm5^{k6801};gkdm5 JmjC*-HA (abbreviation: kdm5^{Jmjc*})* relative to *kdm5^{k6801};gkdm5-HA* flies.

B. *Lactobacillus* spp. bacteria abundance in 3–5 day old *kdm5^{k6801};gkdm5-HA* and *kdm5^{JmJC*}* mutant flies.

C. Real-time PCR analysis of abundance of *L. plantarum* L168 and *P. rettgeri P6* in *kdm5^{JmjC*}*and *kdm5^{k6801};gkdm5-HA* flies.

D. Number of PH3 positive staining cells in mid-gut from *kdm5^{JmjC*}* and *kdm5^{k6801};gkdm5-HA* flies. 10–20 flies each group were examined at the 3–5 days.

E. Intestinal permeability analysis for 3–5 day old *kdm5^{k6801};gkdm5-HA* and *kdm5^{JmJC*}* flies was assessed (top-panel). Quantification of the percentage of body area with distribution of non-absorbable blue food dye relative to whole body (bottom-panel).

F. The digestive tract of *kdm5*^{JmjC*} flies are highly permeable. FITC-labeled beads remained in the lumen of *kdm5*^{k6801}*;gkdm5-HA* flies. In contrast, FITC signals were diffuse in the gut of *kdm5*^{JmjC*}flies.

G. Social space in *kdm5*^{JmjC*} and *kdm5*^{k6801}*;gkdm5-HA* flies.

H. Social avoidance activity (performance index) in *kdm5*^{JmjC*} and *kdm5*^{k6801}*;gkdm5-HA* flies.

I. Intestinal permeability in *kdm5*^{JmjC*}flies treated with or without *L. plantarum* L168.

J. Social space in *kdm5*^{JmjC*} flies treated with or without *L. plantarum* L168.

K. Social avoidance (performance index) in *kdm5*^{JmjC*} flies treated with or without *L. plantarum* L168.

L. Concentration of 5-HT in abdomens tissues from *kdm5*^{JmjC*} and *kdm5*^{k6801}*;gkdm5-HA* flies.

M. Concentration of 5-HT in abdomens tissues from *kdm5*^{JmjC*} flies treated with or without *L. plantarum* L168.

Error bars represent min and max (G and J). Data are shown as mean ± SEM. n≥3 (B and G-M). n=2 (A and C). Data shown in D-F are representative of two independent experiments. *$P < 0.05$; **$P < 0.01$ and ***$P < 0.001$.

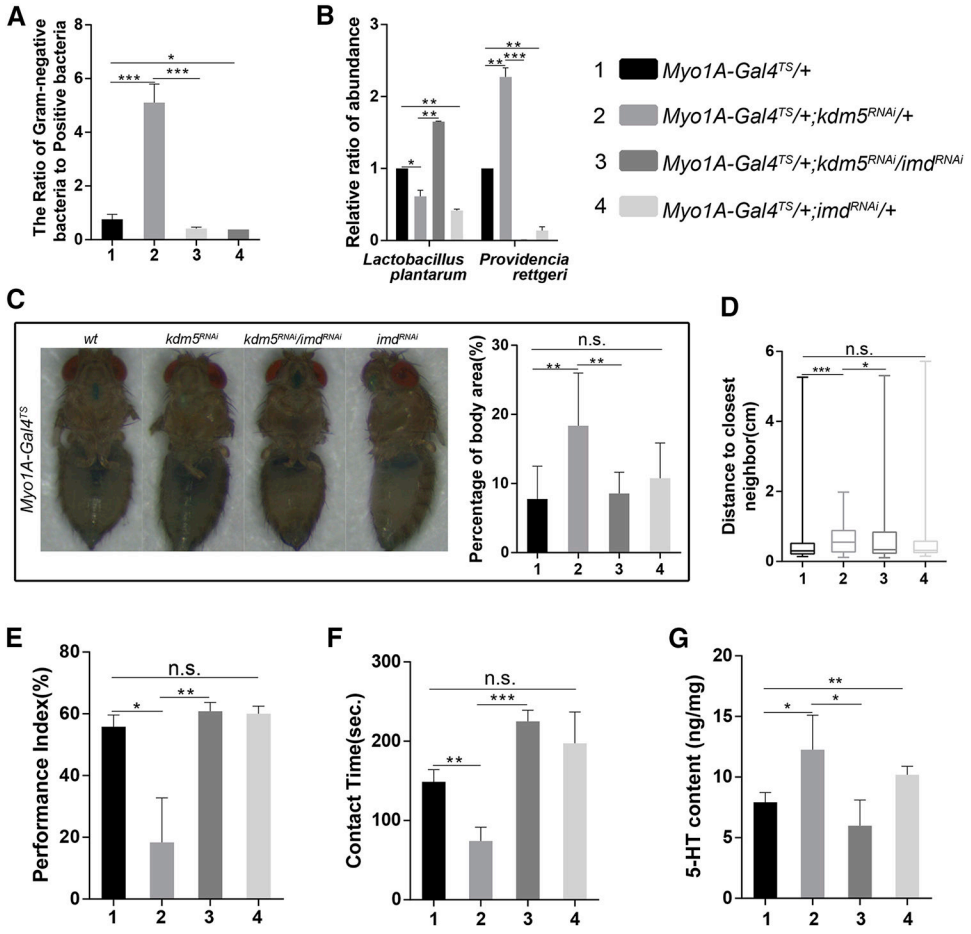

Figure 7. Inhibition of IMD signaling rescues gut dysbiosis and social behavior induced by loss of KDM5

A. The ratio of Gram-negative to Gram-positive bacteria in the gut of four groups.

B. Real-time PCR analysis of abundance of *L. plantarum* L8168 and *P. rettgeri P6* in gut tissue from four groups.

C. Intestinal permeability in four groups was assessed (left panel). Quantification of the percentage of body area with distribution of non-absorbable blue food dye relative to whole body (right panel).

D. Social space analysis in four groups.

E. Social avoidance (performance index) in four groups.

F. Direct social contacting time in four groups flies.

G. Concentration of 5-HT in body from four groups flies.

The genotypes of the four groups represented in Figures A-G are as follows: *1. Myo1A-Gal4^{TS}/+*. 2. *Myo1A-Gal4^{TS}/+;kdm5^{RNAi}/+*. 3. *Myo1A-Gal4^{TS}/+; kdm5^{RNAi}/imcf^{RNAi}*. 4. *Myo1A-Gal4^{TS}+;imd^{RNAi}/+*. Error bars represent min and max (D). Other data are shown as mean ± SEM; n ≥ 3 (A, D-G). n=2 (B). Data shown in C are representative of two independent experiments. *$P < 0.05$; **$P < 0.01$ and ***$P < 0.001$.